Numer Algor (2017) 74:427–459
DOI 10.1007/s11075-016-0154-3

ORIGINAL PAPER

Numerov type variable mesh approximations for 1D unsteady quasi-linear biharmonic problem: application to Kuramoto-Sivashinsky equation

R. K. Mohanty[1] · **Deepti Kaur**[2]

Received: 8 November 2015 / Accepted: 24 May 2016 / Published online: 8 June 2016

Abstract We present two new two-level compact implicit variable mesh numerical methods of order two in time and two in space, and of order two in time and three in space for the solution of 1D unsteady quasi-linear biharmonic problem subject to suitable initial and boundary conditions. The simplicity of the proposed methods lies in their three-point discretization without requiring any fictitious points for incorporating the boundary conditions. The derived methods are shown to be unconditionally stable for a model linear problem for uniform mesh. We also discuss how our formulation is able to handle linear singular problem and ensure that the developed numerical methods retain their orders and accuracy everywhere in the solution region. The proposed difference methods successfully works for the highly nonlinear Kuramoto-Sivashinsky equation. Many physical problems are solved to demonstrate the accuracy and efficiency of the proposed methods. The numerical results reveal that the obtained solutions not only approximate the exact solutions very well but are also much better than those available in earlier research studies.

Keywords Unsteady quasi-linear biharmonic problem · Variable mesh finite difference methods · Singular equation · Generalized fourth-order KdV equation · Kuramoto-Sivashinsky equation · Extended Fisher-Kolmogorov equation

Mathematics Subject Classifications (2010) 65M06 · 65M12 · 65M22

✉ R. K. Mohanty
rmohanty@sau.ac.in

[1] Department of Applied Mathematics, Faculty of Mathematics and Computer Science, South Asian University, Akbar Bhawan, Chanakyapuri, New Delhi 110021, India

[2] Department of Mathematics, Faculty of Mathematical Sciences, University of Delhi, Delhi 110007, India

1 Introduction

We consider the following fourth-order quasi-linear partial differential equation (PDE) of the form:

$$A(x,t,u,u_{xx})\frac{\partial^4 u}{\partial x^4}+\frac{\partial u}{\partial t}=f(x,t,u,u_x,u_{xx},u_{xxx}), \tag{1}$$

where $(x,t)\in\Omega\equiv\{(x,t)|\,a<x<b,\ t>0\}$, or equivalently, by defining a new variable v as $v=\dfrac{\partial^2 u}{\partial x^2}$, the above problem may be considered in a coupled manner as:

$$\frac{\partial^2 u}{\partial x^2}=v,\quad (x,t)\in\Omega, \tag{2.1}$$

$$A(x,t,u,v)\frac{\partial^2 v}{\partial x^2}+\frac{\partial u}{\partial t}=f(x,t,u,v,u_x,v_x),\quad (x,t)\in\Omega, \tag{2.2}$$

subject to the following initial and boundary conditions:

$$u(x,0)=u_0(x),\quad a\le x\le b, \tag{3.1}$$

$$u(a,t)=g_0(t),\quad u(b,t)=g_1(t),\quad t>0, \tag{3.2}$$

$$u_{xx}(a,t)=v(a,t)=h_0(t),\quad u_{xx}(b,t)=v(b,t)=h_1(t),\quad t>0, \tag{3.3}$$

where u_0, g_0, g_1, h_0, and h_1 are functions of sufficient smoothness and their required higher order derivatives exist in the solution region Ω. The PDE (1) together with the initial and boundary conditions (3.1)–(3.3) is referred as 1D unsteady quasi-linear biharmonic problem of second kind.

Nonlinear unsteady biharmonic problems model many physical phenomena and dynamic processes in science and engineering. Major nonlinear PDEs of type (1) which occur in a wide variety of physical problems are considered in our study. Included are generalized fourth-order Korteweg-de Vries (KdV) equation, generalized Kuramoto-Sivashinsky (GKS) equation, and the extended Fisher-Kolmogorov (EFK) equation. The methods proposed in this study are applicable to these equations whose spatial domain $a<x<b$ is a finite interval of $\mathbb{R}$ subject to initial and boundary conditions prescribed by (3.1)–(3.3). Korteweg and de Vries [15] originally introduced KdV equation to model complex phenomena of solitons. It is a classical nonlinear PDE in physics formulated to model dispersive wave phenomena in the theory of solids, liquids, gases, and plasma [15]. In this paper, we consider the following generalized fourth-order KdV equation of the form:

$$\frac{\partial^4 u}{\partial x^4}+\frac{\partial u}{\partial t}+(p+1)u^p u_x=0,\quad p>2,\quad (x,t)\in\Omega. \tag{4}$$

Other important 1D unsteady biharmonic problem considered in the paper is the GKS equation given by

$$\frac{\partial u}{\partial t}+u\frac{\partial u}{\partial x}+\alpha\frac{\partial^2 u}{\partial x^2}+\beta\frac{\partial^3 u}{\partial x^3}+\gamma\frac{\partial^4 u}{\partial x^4}=0,\quad (x,t)\in\Omega, \tag{5}$$

where α, β, and γ are real constants. It is a model of nonlinear PDE encountered commonly in the study of continuous media that displays a chaotic behavior form.

It arises in a broad spectrum of contexts such as unstable drift waves in plasma, stationary solitary pulses in a falling film and can be applied to describe stress waves in fragmented porous media (see [24, 27]). The GKS equation without the third-order derivative term is called the Kuramoto-Sivashinsky (KS) equation:

$$\frac{\partial u}{\partial t} + u\frac{\partial u}{\partial x} + \alpha\frac{\partial^2 u}{\partial x^2} + \gamma\frac{\partial^4 u}{\partial x^4} = 0, \quad (x,t) \in \Omega. \tag{6}$$

The KS equation is a canonical nonlinear PDE occurring in numerous physical frameworks, for instance in reaction diffusion systems [16], long waves on the interface between two viscous fluids [10], and flame front instability [25]. It occupies a significant position in explaining the motion of a fluid going down a vertical wall, a spatially uniform oscillating chemical reaction in a homogeneous medium and unstable drift waves in plasmas [2]. It is the simplest PDE which is capable of exhibiting chaotic behavior, possessing solution like traveling waves which progress without varying shape over a finite spatial domain, see [7, 18, 20, 28]. Over the last few decades, the KS equation has attracted great attention owing to its intricacy and ability to express real world processes. Another time-dependent fourth-order PDE tested in the paper is the EFK equation:

$$\frac{\partial u}{\partial t} + \gamma\frac{\partial^4 u}{\partial x^4} - \frac{\partial^2 u}{\partial x^2} + f(u) = 0, \quad (x,t) \in \Omega, \tag{7}$$

where $f(u) = u^3 - u$. The EFK equation was first proposed by Dee and Van Saarlos [4] as a higher order model equation arising in the study of pattern formation in bistable systems. It has a large variety of applications in the theory of propagation of domain walls in liquid crystals [31] and traveling waves in reaction-diffusion systems [1].

The analytical treatment of nonlinear PDEs unlike their linear counterparts is too involved a process and requires application of advanced mathematical tools. It is not usually possible to determine closed-form solutions of nonlinear time-dependent PDEs, even in very simple cases. Therefore, numerical techniques for finding approximate solutions to these PDEs are sought after. Over a last few decades, there has been considerable amount of research aiming to find methods for numerical solutions of PDEs of type (1). A number of explicit and implicit difference schemes for the linear 1D unsteady biharmonic problem have been reported since 1950. In 1969, Mitchell [19] gave an explicit difference scheme for the PDE (1) with $A = 1,\ f = 0$. Approximate solutions of the fourth-order KdV equation have been undertaken by employing various forms of pseudo-spectral methods, finite difference techniques, and finite element methods [8, 26, 29]. Earlier, in 2005, Kaya [11] calculated explicit solutions to the fourth-order KdV equation using the Adomian decomposition method, without spatial discretizations. In recent years, several methods have been proposed for numerical study of the GKS equation, for example, tanh-function method [6], local discontinuous Galerkin method [30], and Chebyshev spectral collocation method [13]. Later, in 2009, Lai and Ma [17] proposed a lattice Boltzmann model, a technique different from conventional numerical methods for the GKS equation. Recently, Lakestani and Dehghan [18] designed a numerical procedure based on the finite difference and collocation methods for the solution of the GKS equation. An accurate

and efficient approach for the numerical solution of KS equation was presented by Uddin et al. [28] by implementing radial basis function based mesh-free interpolation method which is applicable irrespective of the dimension and geometry of the problem. Further, Mittal and Arora [20] gave a numerical treatment for the KS equation using a collocation method with the quintic B-spline functions. Most recently, Ganaie et al. [7] employed cubic Hermite functions to develop a collocation method for the numerical solution of KS equation and derived a bound for maximum norm of the semi-discrete solution using Lyapunov functional. As far as computational studies for the EFK equation are concerned, Danumjaya and Pani [3] performed some numerical experiments to obtain approximate solution using orthogonal cubic spline collocation method. Doss and Nandini [5] presented a study on numerical implementation of the H^1-Galerkin mixed finite element cubic spline approximation method for the EFK equation by using a splitting technique.

It is quite challenging to find the numerical solution of 1D unsteady nonlinear biharmonic problems like the KS equation, the EFK equation and the fourth-order KdV equation due to their extremely complex mechanism of solitary wave interaction. Of late, the use of high-order compact finite difference methods for the computation of such equations are steadily acquiring popularity owing to their high accuracy and the advantages related with compact cell. In this regard, Mohanty [21] discussed two-level implicit difference formulas of $O(k^2 + h^2)$ and $O(k^2 + h^4)$, where $k > 0$ and $h > 0$ are the mesh sizes in the temporal and spatial dimensions, respectively, of a uniform mesh for the solution of one-space dimensional mildly quasi-linear biharmonic problems of second kind on a compact difference stencil. Most recently, Mohanty and Kaur [22] have proposed two new two-level and three-level implicit finite difference methods of $O(k^2 + kh_l + h_l^3)$ and $O(k^2 + h_l^3)$ where $h_l > 0$, $l = 1, 2, \ldots, N + 1$ are mesh sizes in space dimension of a non-uniform mesh for two different classes of nonlinear fourth-order parabolic PDEs using three spatial non-uniform grid points, which were successfully applied to the second-order Benjamin-Ono equation and the good Boussinesq equation. In the present article, we propose new and accurate two-level implicit variable mesh finite difference formulas of $O(k^2 + h_l^2)$ and $O(k^2 + kh_l + h_l^3)$ based on the approach discussed in [22] by reducing the fourth-order equation to a coupled system of two second-order equations using Numerov type discretization requiring only three spatial non-uniform grid points at each time level. In this approach, no fictitious points for incorporating the boundary conditions are required. The conventional finite difference schemes for the problem (1) subject to (3.1)–(3.3) are based on five or more grid points and thus needs fictitious points outside the solution domain. These fictitious points are then eliminated by discretizing the derivative boundary conditions (3.3). However, using the second-order central differences for the boundary conditions (3.3), the accuracy of the overall numerical scheme is affected even if a higher order scheme is used at internal grid points. The numerical algorithm proposed in the present paper decompose the fourth-order equation into a coupled elliptic-parabolic pair and is advantageous over the traditional schemes as it systematically incorporates the derivative boundary conditions without discretization. It achieves high order of accuracy by using only three grid points at each time level. In the proposed methods, numerical solution of u_{xx} is computed as a by-product of the methods, which is of relative importance in

many physical problems. In the past, difficulties were encountered to determine the numerical solution of singular equation of type (1) since the solution deteriorates in the neighbourhood of singularity. We overcome this difficulty by amending our methods in such a way that the order and accuracy of the solution is retained everywhere including the region in the neighborhood of singularity. The main aim of this article is the application of the proposed high accuracy schemes to the model problems like the KS equation, the EFK equation and the fourth-order KdV equation. With this reason, we first develop the new schemes and further apply them to these problems of physical significance.

The rest of this paper is organized as follows: In Section 2, we present two new two-level implicit variable mesh difference methods for 1D unsteady quasi-linear biharmonic problem of second kind, which are further derived in Section 3. In Section 4, linear stability analysis of the proposed methods is carried out and it is shown that the methods are unconditionally stable. In this section, we discuss how our formulation is able to handle singular equation by modifying our technique in such a way that the solution retains its order and accuracy everywhere in the solution region. In Section 5, we implement the proposed methods on some problems of physical importance and compare the results with the results of other known methods available in the literature. It is shown that the proposed schemes produce better accuracy as compared to the techniques given in earlier studies. Some concluding remarks are given in Section 6.

2 Formulation of new variable mesh methods

In this section, we outline variable mesh difference methods for the solution of differential equation (1).

For simplicity, let us first consider 1D unsteady nonlinear biharmonic problem of the form:

$$A(x,t)\frac{\partial^4 u}{\partial x^4} + \frac{\partial u}{\partial t} = f(x,t,u,u_x,u_{xx},u_{xxx}), \quad (x,t) \in \Omega, \tag{8}$$

or equivalently,

$$\frac{\partial^2 u}{\partial x^2} = v, \quad (x,t) \in \Omega, \tag{9.1}$$

$$A(x,t)\frac{\partial^2 v}{\partial x^2} + \frac{\partial u}{\partial t} = f(x,t,u,v,u_x,v_x), \quad (x,t) \in \Omega, \tag{9.2}$$

subject to the initial and boundary conditions given by (3.1)–(3.3).

Note that at $x = a$ and $x = b$, the values of u and v are given by (3.2) and (3.3), respectively. Using the initial condition (3.1), the values of all the successive tangential partial derivatives $u_x, u_{xx}, \ldots,$ of u can be determined at $t = 0$. Since $v(x,0) = u_{xx}(x,0)$, so the value of v is also known at $t = 0$. Hence, the values of u and v are known on all sides of the solution region Ω.

To obtain the numerical solution of the initial boundary value problem given by (9.1)–(9.2) subject to (3.1)–(3.3) on a variable mesh, we partition the interval $[a,b]$

into $(N+1)$ subintervals such that $a = x_0 < x_1 < \ldots < x_N < x_{N+1} = b$, where N is a positive integer. The temporal interval is split as $0 = t_0 < t_1 < \ldots < t_J = T$, where J is a positive integer and T is defined as the final time of the computation. Let $k = t_{j+1} - t_j > 0$, $j = 0, 1, \ldots, J-1$ be the mesh length for the temporal variable t, so that $k = T/J$ and $h_l = x_l - x_{l-1} > 0$ be the mesh lengths for the spatial variable x, where $l = 1, 2, \ldots, N+1$. Hence, the solution region Ω is covered by a rectangular mesh in which each mesh point is denoted by (x_l, t_j), with $x_l = x_0 + \Sigma_{i=1}^{l} h_i$, $l = 1, 2, \ldots, N+1$ and $t_j = jk$, $j = 0, 1, \ldots, J$. The mesh ratio is denoted by $\eta_l = (h_{l+1}/h_l) > 0, l = 1, 2, \ldots, N$. For $\eta_l = 1$, that is, for $h_{l+1} = h_l = h$, it reduces to the uniform mesh case. Let the exact solution values of $u(x,t)$ and $v(x,t)$ at the mesh point (x_l, t_j) be denoted by U_l^j and V_l^j, respectively, and u_l^j and v_l^j denote their approximate solution values, respectively. For the sake of simplicity, we consider $\eta_l = \eta$ (a constant $\neq 1$), $l = 1, 2, \ldots, N$.

In order to obtain the high accuracy Numerov type discretization of the differential (9.1)–(9.2), we need the following approximations:

For $r = 0, \pm 1$, let us denote

$$\bar{t}_j = t_j + \theta k, \quad 0 < \theta < 1, \tag{10.1}$$

$$\overline{A}_l^j = A(x_l, \bar{t}_j), \tag{10.2}$$

$$\overline{A}_{x_l}^j = A_x(x_l, \bar{t}_j), \tag{10.3}$$

$$\overline{A}_{xx_l}^j = A_{xx}(x_l, \bar{t}_j), \tag{10.4}$$

$$\overline{U}_{l+r}^j = \theta U_{l+r}^{j+1} + (1-\theta) U_{l+r}^j, \tag{10.5}$$

$$\overline{V}_{l+r}^j = \theta V_{l+r}^{j+1} + (1-\theta) V_{l+r}^j, \tag{10.6}$$

$$\overline{U}_{t_{l+r}}^j = (U_{l+r}^{j+1} - U_{l+r}^j)/k, \tag{10.7}$$

$$\overline{U}_{x_l}^j = (\overline{U}_{l+1}^j - (1-\eta^2)\overline{U}_l^j - \eta^2 \overline{U}_{l-1}^j)/(\eta(1+\eta)h_l), \tag{10.8}$$

$$\overline{U}_{x_{l+1}}^j = ((1+2\eta)\overline{U}_{l+1}^j - (1+\eta)^2 \overline{U}_l^j + \eta^2 \overline{U}_{l-1}^j)/(\eta(1+\eta)h_l), \tag{10.9}$$

$$\overline{U}_{x_{l-1}}^j = (-\overline{U}_{l+1}^j + (1+\eta)^2 \overline{U}_l^j - \eta(2+\eta)\overline{U}_{l-1}^j)/(\eta(1+\eta)h_l), \tag{10.10}$$

$$\overline{V}_{x_l}^j = (\overline{V}_{l+1}^j - (1-\eta^2)\overline{V}_l^j - \eta^2 \overline{V}_{l-1}^j)/(\eta(1+\eta)h_l), \tag{10.11}$$

$$\overline{V}_{x_{l+1}}^j = ((1+2\eta)\overline{V}_{l+1}^j - (1+\eta)^2 \overline{V}_l^j + \eta^2 \overline{V}_{l-1}^j)/(\eta(1+\eta)h_l), \tag{10.12}$$

$$\overline{V}_{x_{l-1}}^j = (-\overline{V}_{l+1}^j + (1+\eta)^2 \overline{V}_l^j - \eta(2+\eta)\overline{V}_{l-1}^j)/(\eta(1+\eta)h_l), \tag{10.13}$$

$$\overline{V}_{xx_l}^j = 2(\overline{V}_{l+1}^j - (1+\eta)\overline{V}_l^j + \eta \overline{V}_{l-1}^j)/(\eta(1+\eta)h_l^2). \tag{10.14}$$

For $r = 0$, the approximations are defined at $(x_l, \bar{t}_j)$ and for $r = \pm 1$, the approximations are defined at two neighboring points $(x_{l\pm1}, \bar{t}_j)$.

At the mesh point (x_l, t_j), we denote

$$P_{1_l} = \frac{(\eta-1)}{3} - \frac{h_l}{18}(1+\eta+\eta^2)\frac{\overline{A}^j_{x_l}}{\overline{A}^j_l}, \tag{11.1}$$

$$P_{2_l} = \frac{1-\eta+\eta^2}{12}, \tag{11.2}$$

$$P_l = \eta^2+\eta-1-\frac{h_l}{3}(1+\eta+\eta^2)\frac{\overline{A}^j_{x_l}}{\overline{A}^j_l}, \tag{11.3}$$

$$Q_l = (1+\eta)(1+3\eta+\eta^2) + \frac{h_l}{3}(1-\eta^2)(1+\eta+\eta^2)\frac{\overline{A}^j_{x_l}}{\overline{A}^j_l}, \tag{11.4}$$

$$R_l = \eta(1+\eta-\eta^2) + \frac{h_l}{3}\eta^2(1+\eta+\eta^2)\frac{\overline{A}^j_{x_l}}{\overline{A}^j_l}. \tag{11.5}$$

Using the approximations (10.1) and (10.5)–(10.13), we define

$$\overline{F}^j_{l+r} = f(x_{l+r}, \bar{t}_j, \overline{U}^j_{l+r}, \overline{V}^j_{l+r}, \overline{U}^j_{x_{l+r}}, \overline{V}^j_{x_{l+r}}). \tag{12}$$

In order to achieve high-order accuracy of the first-order partial derivatives of the solution variables at the concerned point $(x_l, \bar{t}_j)$, we consider the following linear combinations:

$$\overline{\overline{U}}^j_{x_l} = \overline{U}^j_{x_l} + a_1 h_l(\overline{V}^j_{l+1} - \overline{V}^j_{l-1}), \tag{13.1}$$

$$\overline{\overline{V}}^j_{x_l} = \overline{V}^j_{x_l} + b_1 h_l[(\overline{F}^j_{l+1} - \overline{F}^j_{l-1}) - (\overline{U}^j_{t_{l+1}} - \overline{U}^j_{t_{l-1}})] + b_2 h_l^2 \overline{V}^j_{xx_l}, \tag{13.2}$$

where a_1, b_1, and b_2 are the parameters to be suitably determined.

The additional approximation to the first-order derivatives are then applied to obtain the functional value at the point $(x_l, \bar{t}_j)$, defined by the relation

$$\overline{\overline{F}}^j_l = f(x_l, \bar{t}_j, \overline{U}^j_l, \overline{V}^j_l, \overline{\overline{U}}^j_{x_l}, \overline{\overline{V}}^j_{x_l}). \tag{14}$$

Then, at each internal mesh point (x_l, t_j), $l = 1, 2, \ldots, N$, $j = 0, 1, \ldots, J$, the differential equations (9.1)–(9.2) are discretized by finite difference methods of $O(k^2+h_l^2)$ and $O(k^2+kh_l+h_l^3)$ given by

$$\overline{U}^j_{l+1} - (1+\eta)\overline{U}^j_l + \eta\overline{U}^j_{l-1} = \frac{h_l^2}{6}[(\eta-1)\overline{V}^j_{l+1} + (1+\eta)(1+\eta+\eta^2)\overline{V}^j_l - \eta^2(\eta-1)\overline{V}^j_{l-1}] + O(k^2h_l^2 + kh_l^3 + h_l^4), \tag{15.1}$$

$$[\overline{A}^j_l + \frac{(\eta-1)}{3}h_l\overline{A}^j_{x_l}](\overline{V}^j_{l+1} - (1+\eta)\overline{V}^j_l + \eta\overline{V}^j_{l-1}) + \frac{h_l^2}{6}[(\eta-1)\overline{U}^j_{t_{l+1}} + (1+\eta)(1+\eta+\eta^2)\overline{U}^j_{t_l} - \eta^2(\eta-1)\overline{U}^j_{t_{l-1}}] = \frac{h_l^2}{6}[(\eta-1)\overline{F}^j_{l+1} + (1+\eta)(1+\eta+\eta^2)\overline{F}^j_l - \eta^2(\eta-1)\overline{F}^j_{l-1}] + O(k^2h_l^2 + kh_l^3 + h_l^4), \quad \eta \neq 1, \tag{15.2}$$

and

$$\overline{U}_{l+1}^j-(1+\eta)\overline{U}_l^j+\eta\overline{U}_{l-1}^j=\frac{h_l^2}{12}[(\eta^2+\eta-1)\overline{V}_{l+1}^j+(1+\eta)(1+3\eta+\eta^2)\overline{V}_l^j$$
$$+\eta(1+\eta-\eta^2)\overline{V}_{l-1}^j]+\overline{T}_l^{j\,(1)},\tag{16.1}$$

$$[\overline{A}_l^j+h_lP_{1_l}\overline{A}_{x_l}^j+h_l^2P_{2_l}\overline{A}_{xx_l}^j](\overline{V}_{l+1}^j-(1+\eta)\overline{V}_l^j+\eta\overline{V}_{l-1}^j)+\frac{h_l^2}{12}[P_l\overline{U}_{t_{l+1}}^j+Q_l\overline{U}_{t_l}^j+R_l\overline{U}_{t_{l-1}}^j]$$
$$=\frac{h_l^2}{12}[P_l\overline{F}_{l+1}^j+Q_l\overline{\overline{F}}_l^j+R_l\overline{F}_{l-1}^j]+\overline{T}_l^{j\,(2)},\quad \eta\neq 1,\tag{16.2}$$

respectively, where

$$\theta=\frac{1}{2},\quad a_1=\frac{-\eta(1+\eta+\eta^2)}{6Q_l}\left(1+\frac{2(1-\eta)h_l\overline{A}_{x_l}^j}{3\overline{A}_l^j}\right),$$
$$b_1=\frac{-\eta(1+\eta+\eta^2)}{6\overline{A}_l^jQ_l}\left(1+\frac{2(1-\eta)h_l\overline{A}_{x_l}^j}{3\overline{A}_l^j}\right),$$
$$b_2=\frac{\eta(1+\eta)(1+\eta+\eta^2)\overline{A}_{x_l}^j}{6\overline{A}_l^jQ_l}\left(1+\frac{2(1-\eta)h_l\overline{A}_{x_l}^j}{3\overline{A}_l^j}\right),$$

and $\overline{T}_l^{j\,(1)}=O(k^2h_l^2+kh_l^3+h_l^5)$, $\overline{T}_l^{j\,(2)}=O(k^2h_l^2+kh_l^3+h_l^5)$, provided $\eta\neq 1$.

The methods (15.1)–(15.2) and (16.1)–(16.2) are called *two-level* methods. These methods give a relation between the solution values at two time levels $t_{j+1}=t_j+k$ and t_j. The solution value at any nodal point on $(j+1)$th level is dependent on the solution values at the neighboring nodal points $(x_{l\pm1},t_{j+1})$ on the same level and on the solution values at three nodal points (x_l,t_j), $(x_{l\pm1},t_j)$ on the jth level.

For the quasi-linear differential (2.1)–(2.2), i.e., when the coefficient $A=A(x,t,u,v)$, then we need to modify our proposed difference methods (15.1)–(15.2) and (16.1)–(16.2). In this case, we make use of the following approximations in (15.1)–(15.2) and (16.1)–(16.2):

$$\overline{A}_{x_l}^j=\frac{\overline{A}_{l+1}^j-(1-\eta^2)\overline{A}_l^j-\eta^2\overline{A}_{l-1}^j}{\eta(1+\eta)h_l},\tag{17.1}$$

$$\overline{A}_{xx_l}^j=\frac{2(\overline{A}_{l+1}^j-(1+\eta)\overline{A}_l^j+\eta\overline{A}_{l-1}^j)}{\eta(1+\eta)h_l^2},\tag{17.2}$$

where

$$\overline{A}_l^j=A(x_l,\bar{t}_j,\overline{U}_l^j,\overline{V}_l^j),\tag{17.3}$$

$$\overline{A}_{l\pm1}^j=A(x_{l\pm1},\bar{t}_j,\overline{U}_{l\pm1}^j,\overline{V}_{l\pm1}^j).\tag{17.4}$$

Substituting (17.1)–(17.2) using (17.3)–(17.4) into the original schemes (15.1)–(15.2) and (16.1)–(16.2), we obtain two new finite difference formulas of $O(k^2+kh_l+h_l^3)$ and $O(k^2+h_l^2)$, respectively. Incorporating the initial and boundary conditions (3.1)–(3.3), the new implicit finite difference methods can be expressed in two-level block tri-diagonal matrix form which can be solved by suitable iterative

methods. If the differential (1) is linear, then we use Gauss-Seidel iteration method whereas for the nonlinear case, we use Newton's nonlinear block iteration method (see Hageman and Young [9]).

3 Derivation of the discretizations

In this section, we discuss the derivation procedure of the novel second-order formula (15.1)–(15.2) and the novel Numerov type discretization given by (16.1)–(16.2) on a variable mesh following the techniques proposed by Mohanty and Kaur [22].

In order to illustrate the general procedure used for constructing the difference formulas (15.1)–(15.2) and (16.1)–(16.2) to the equations (9.1)–(9.2), we first consider the simplest form of the second-order ordinary differential equation:

$$A(x)u''(x) = f(x). \tag{18}$$

For the second-order method to (18), we consider

$$F_l + h_l M^*_{1_l} F'_l = (A_l + h_l M^*_{1_l} A'_l)U''_l + M^*_{1_l} A_l h_l U'''_l, \tag{19}$$

where the exact solution value of $u(x)$ at the grid point x_l is denoted by U_l and $F_l = f(x_l)$, $A_l = A(x_l)$, $A'_l = A'(x_l)$ etc. and $M^*_{1_l}$ is a parameter to be determined suitably.

Consider the following approximation

$$\begin{aligned} \overline{U}''_l &= 2(U_{l+1} - (1+\eta)U_l + \eta U_{l-1})/(\eta(1+\eta)h_l^2) \\ &= U''_l + \frac{(\eta-1)}{3}h_l U'''_l + \frac{(1-\eta+\eta^2)}{12}h_l^2 U_l^{\mathrm{iv}} + O(h_l^3). \end{aligned} \tag{20}$$

Using the approximation (20) in (19), we obtain

$$F_l + h_l M^*_{l_l} F'_l = (A_l + h_l M^*_{1_l} A'_l)\overline{U}''_l + \left(M^*_{1_l} A_l - \frac{(\eta-1)A_l}{3}\right)h_l U'''_l + O(h_l^2). \tag{21}$$

Equating the coefficient of $h_l U'''_l$ to zero in (21), we get $M^*_{1_l} = \dfrac{\eta-1}{3}$. Substituting the value of $M^*_{1_l}$ back in (21), we obtain

$$\begin{aligned} (A_l + h_l M^*_{1_l} A'_l)\overline{U}''_l &= F_l + h_l M^*_{1_l} F'_l + O(h_l^2) \\ &= F_l + \frac{(\eta-1)}{3}\frac{1}{\eta(1+\eta)}[F_{l+1} - (1-\eta^2)F_l - \eta^2 F_{l-1}] + O(h_l^2), \end{aligned} \tag{22}$$

where the following approximation

$$\overline{F}'_l = \frac{1}{\eta(1+\eta)h_l}[F_{l+1} - (1-\eta^2)F_l - \eta^2 F_{l-1}] = F'_l + O(h_l^2), \tag{23}$$

is used. This leads to the following scheme:

$$[A_l + \frac{(\eta-1)}{3}h_l A_l'](U_{l+1} - (1+\eta)U_l + \eta U_{l-1})$$
$$= \frac{h_l^2}{6}[(\eta-1)F_{l+1} + (1+\eta)(1+\eta+\eta^2)F_l - \eta^2(\eta-1)F_{l-1}] + O(h_l^2). \quad (24)$$

For the third-order method to (18), consider

$$F_l + h_l M_{1_l} F_l' + h_l^2 M_{2_l} F_l'' = (A_l + h_l M_{1_l} A_l' + h_l^2 M_{2_l} A_l'')U_l'' + (M_{l_l} A_l + 2h_l M_{2_l} A_l')h_l U_l''' + M_{2_l} A_l h_l^2 U_l^{\mathrm{iv}}, \quad (25)$$

where M_{1_l} and M_{2_l} are the parameters to be obtained suitably. Using the approximation (20) in (25), we obtain

$$F_l + h_l M_{1_l} F_l' + h_l^2 M_{2_l} F_l'' = (A_l + h_l M_{1_l} A_l' + h_l^2 M_{2_l} A_l'')\overline{U}_l''$$
$$+\left(M_{1_l} A_l + 2h_l M_{2_l} A_l' - \frac{(\eta-1)}{3}(A_l + h_l M_{1_l} A_l'')\right)h_l U_l'''$$
$$+\left(M_{2_l} A_l - \frac{(1-\eta+\eta^2)}{12}A_l\right)h_l^2 U_l^{\mathrm{iv}} + O(h_l^3). \quad (26)$$

Equating the coefficients of $h_l U_l'''$ and $h_l^2 U_l^{\mathrm{iv}}$ to zero in (26), we obtain

$$M_{1_l} = \frac{(\eta-1)}{3} - \frac{h_l}{18}(1+\eta+\eta^2)\frac{A_l'}{A_l},$$
$$M_{2_l} = \frac{1-\eta+\eta^2}{12}.$$

Also,

$$\overline{F}_l'' = 2(F_{l+1} - (1+\eta)F_l + \eta F_{l-1})/(\eta(1+\eta)h_l^2)$$
$$= F_l'' + \frac{(\eta-1)}{3}h_l F_l''' + \frac{(1-\eta+\eta^2)}{12}h_l^2 F_l^{\mathrm{iv}} + O(h_l^3). \quad (27)$$

Substituting the values of M_{1_l}, M_{2_l} back in (26) and using the relations (23) and (27), we get

$$(A_l + h_l M_{1_l} A_l' + h_l^2 M_{2_l} A_l'')\overline{U}_l''$$
$$= F_l + h_l M_{1_l} F_l' + h_l^2 M_{2_l} F_l'' + O(h_l^3)$$
$$= F_l + \left(\frac{(\eta-1)}{3} - \frac{h_l}{18}(1+\eta+\eta^2)\frac{A_l'}{A_l}\right)\frac{1}{\eta(1+\eta)}[F_{l+1} - (1-\eta^2)F_l - \eta^2 F_{l-1}]$$
$$+\frac{(1-\eta+\eta^2)}{12}\frac{2}{\eta(1+\eta)}(F_{l+1} - (1+\eta)F_l + \eta F_{l-1}) + O(h_l^3), \quad (28)$$

which gives the following scheme

$$[A_l + h_l M_{1_l} A_l' + h_l^2 M_{2_l} A_l'](U_{l+1} - (1+\eta)U_l + \eta U_{l-1}) = \frac{h_l^2}{12}[L_l F_{l+1} + M_l F_l + N_l F_{l-1}]$$
$$+O(h_l^3), \quad (29)$$

where

$$L_l = \eta^2 + \eta - 1 - \frac{h_l}{3}(1+\eta+\eta^2)\frac{A_l'}{A_l},$$
$$M_l = (1+\eta)(1+3\eta+\eta^2) + \frac{h_l}{3}(1-\eta^2)(1+\eta+\eta^2)\frac{A_l'}{A_l},$$
$$N_l = \eta(1+\eta-\eta^2) + \frac{h_l}{3}\eta^2(1+\eta+\eta^2)\frac{A_l'}{A_l}.$$

The basic schemes (24) and (29) are used to obtain the difference formulas (15.1)–(15.2) and (16.1)–(16.2) to the equations (9.1)–(9.2) which involves both temporal and spatial variables. This is accomplished by defining the approximations to u, v, u_t, u_x, v_x given by (10.5), (10.6), (10.7), (10.8)–(10.10), (10.11)–(10.13), respectively, at the point $(x_l, \bar{t}_j)$ and the neighboring points $(x_{l\pm1}, \bar{t}_j)$. Using these approximations, the functional approximations given by (12), the additional approximations (13.1)–(13.2), (14) and following the methods (24) and (29) adopted for the ordinary differential (18), it results in difference formulas (15.1)–(15.2) and (16.1)–(16.2) whose local truncation errors are estimated below.

At the mesh point (x_l, t_j), for $S = A, B, C, D, U, V$ and g, we denote

$$S_{ab} = \frac{\partial^{a+b} S}{\partial x^a \partial t^b}, \quad a, b = 0, 1, 2, \ldots \tag{30}$$

Then, at the mesh point (x_l, t_j), the differential (9.1)–(9.2) may be written as:

$$U_{20} = V_{00}, \tag{31.1}$$
$$A_{00}V_{20} + U_{01} = f(x, t_j, U_l^j, V_l^j, U_{x_l}^j, V_{x_l}^j) \equiv F_l^j. \tag{31.2}$$

Further, at the mesh point (x_l, t_j), we denote

$$\alpha_l^j = \frac{\partial f}{\partial U}, \ \beta_l^j = \frac{\partial f}{\partial V}, \ \gamma_l{}^j = \frac{\partial f}{\partial U_x}, \ \delta_l^j = \frac{\partial f}{\partial V_x}, \ \xi_l^j = \frac{\partial f}{\partial t}.$$

Differentiating the (9.1)–(9.2) with respect to 't' at the mesh point (x_l, t_j), we obtain the following relations:

$$U_{21} = V_{01}, \tag{32.1}$$
$$A_{00}V_{21} + A_{01}V_{20} + U_{02} = \xi_l^j + \alpha_l^j U_{01} + \beta_l^j V_{01} + \gamma_l{}^j U_{11} + \delta_l^j V_{11}. \tag{32.2}$$

Simplifying the approximations (10.1)–(10.14) using Taylor series expansion, we obtain

$$\overline{A}_l^j = A_l^j + \theta k A_{01} + O(k^2), \tag{33.1}$$

$$\overline{A}_{x_l}^j = A_{x_l}^j + \theta k A_{11} + O(k^2), \tag{33.2}$$

$$\overline{A}_{xx_l}^j = A_{xx_l}^j + \theta k A_{21} + O(k^2), \tag{33.3}$$

$$\overline{U}_l^j = U_l^j + \theta k U_{01} + O(k^2), \tag{33.4}$$

$$\overline{U}_{l+1}^j = U_{l+1}^j + \theta k U_{01} + \theta k \eta h_l U_{11} + O(k^2 + k h_l^2), \tag{33.5}$$

$$\overline{U}_{l-1}^j = U_{l-1}^j + \theta k U_{01} - \theta k h_l U_{11} + O(k^2 + k h_l^2), \tag{33.6}$$

$$\overline{V}_l^j = V_l^j + \theta k V_{01} + O(k^2), \tag{33.7}$$

$$\overline{V}_{l+1}^j = V_{l+1}^j + \theta k V_{01} + \theta k \eta h_l V_{11} + O(k^2 + k h_l^2), \tag{33.8}$$

$$\overline{V}_{l-1}^j = V_{l-1}^j + \theta k V_{01} - \theta k h_l V_{11} + O(k^2 + k h_l^2), \tag{33.9}$$

$$\overline{U}_{t\,l}^j = U_{t\,l}^j + \frac{k}{2} U_{02} + O(k^2), \tag{33.10}$$

$$\overline{U}_{t\,l+1}^j = U_{t\,l+1}^j + \frac{k}{2} U_{02} + \frac{k\eta h_l}{2} U_{12} + O(k^2 + k h_l^2), \tag{33.11}$$

$$\overline{U}_{t\,l-1}^j = U_{t\,l-1}^j + \frac{k}{2} U_{02} - \frac{k h_l}{2} U_{12} + O(k^2 + k h_l^2), \tag{33.12}$$

$$\overline{U}_{x\,l}^j = U_{x\,l}^j + \frac{\eta h_l^2}{6} U_{30} + \theta k U_{11} + O(k^2 + k h_l + h_l^3), \tag{33.13}$$

$$\overline{U}_{x\,l+1}^j = U_{x\,l+1}^j - \frac{\eta(1+\eta) h_l^2}{6} U_{30} + \theta k U_{11} + O(k^2 + k h_l + h_l^3), \tag{33.14}$$

$$\overline{U}_{x\,l-1}^j = U_{x\,l-1}^j - \frac{(1+\eta) h_l^2}{6} U_{30} + \theta k U_{11} + O(k^2 + k h_l + h_l^3), \tag{33.15}$$

$$\overline{V}_{x\,l}^j = V_{x\,l}^j + \frac{\eta h_l^2}{6} V_{30} + \theta k V_{11} + O(k^2 + k h_l + h_l^3), \tag{33.16}$$

$$\overline{V}_{x\,l+1}^j = V_{x\,l+1}^j - \frac{\eta(1+\eta) h_l^2}{6} V_{30} + \theta k V_{11} + O(k^2 + k h_l + h_l^3), \tag{33.17}$$

$$\overline{V}_{x\,l-1}^j = V_{x\,l-1}^j - \frac{(1+\eta) h_l^2}{6} V_{30} + \theta k V_{11} + O(k^2 + k h_l + h_l^3), \tag{33.18}$$

$$\overline{V}_{xx_l}^j = V_{xx_l}^j + (\eta - 1)\frac{h_l}{3} V_{30} + O(k + h_l^2). \tag{33.19}$$

Again using Taylor series expansion in (12), we obtain

$$\overline{F}_l^j = F_l^j + k T_1 + \frac{\eta h_l^2}{6} T_2 + O(k^2 + k h_l + h_l^3), \tag{34.1}$$

$$\overline{F}_{l+1}^j = F_{l+1}^j + k T_1 - \frac{\eta(1+\eta) h_l^2}{6} T_2 + O(k^2 + k h_l + h_l^3), \tag{34.2}$$

$$\overline{F}_{l-1}^j = F_{l-1}^j + k T_1 - \frac{(1+\eta) h_l^2}{6} T_2 + O(k^2 + k h_l + h_l^3), \tag{34.3}$$

where

$$T_1 = \theta(\xi_l^j + \alpha_l^j U_{01} + \beta_l^j V_{01} + \gamma_l^j U_{11} + \delta_l^j V_{11}),$$
$$T_2 = \gamma_l^j U_{30} + \delta_l^j V_{30}.$$

Firstly, we determine the local truncation errors associated with the method (15.1)–(15.2). By the help of Taylor series expansion and the relations (31.1)–(31.2), we get

$$U_{l+1}^j - (1+\eta)U_l^j + \eta U_{l-1}^j = \frac{h_l^2}{6}[(\eta-1)V_{l+1}^j + (1+\eta)(1+\eta+\eta^2)V_l^j - \eta^2(\eta-1)V_{l-1}^j] + O(h_l^4), \tag{35.1}$$

$$[A_l^j + \frac{(\eta-1)}{3}h_l A_{x_l}^j](V_{l+1}^j - (1+\eta)V_l^j + \eta V_{l-1}^j) + \frac{h_l^2}{6}[(\eta-1)U_{t_{l+1}}^j + (1+\eta)(1+\eta+\eta^2)U_{t_l}^j - \eta^2(\eta-1)U_{t_{l-1}}^j] = \frac{h_l^2}{6}[(\eta-1)F_{l+1}^j + (1+\eta)(1+\eta+\eta^2)F_l^j - \eta^2(\eta-1)F_{l-1}^j] + O(h_l^4), \quad \eta \neq 1. \tag{35.2}$$

Also, we have

$$\overline{U}_{l+1}^j - (1+\eta)\overline{U}_l^j + \eta\overline{U}_{l-1}^j = U_{l+1}^j - (1+\eta)U_l^j + \eta U_{l-1}^j + \frac{\theta}{2}\eta(1+\eta)kh_l^2 U_{21} + O(kh_l^3 + k^2h_l^2), \tag{36.1}$$

$$[\overline{A}_l^j + \frac{(\eta-1)}{3}h_l\overline{A}_{x_l}^j](\overline{V}_{l+1}^j - (1+\eta)\overline{V}_l^j + \eta\overline{V}_{l-1}^j) + \frac{h_l^2}{6}[(\eta-1)\overline{U}_{t_{l+1}}^j + (1+\eta)(1+\eta+\eta^2)\overline{U}_{t_l}^j - \eta^2(\eta-1)\overline{U}_{t_{l-1}}^j] = [A_l^j + \frac{(\eta-1)}{3}h_l A_{x_l}^j](V_{l+1}^j - (1+\eta)V_l^j + \eta V_{l-1}^j) + \frac{h_l^2}{6}[(\eta-1)U_{t_{l+1}}^j + (1+\eta)(1+\eta+\eta^2)U_{t_l}^j - \eta^2(\eta-1)U_{t_{l-1}}^j] + \frac{\eta(1+\eta)}{2}kh_l^2\big[\theta(A_l^j V_{21} + A_{t_l}^j V_{20}) + \frac{U_{02}}{2}\big] + O(kh_l^3 + k^2h_l^2). \tag{36.2}$$

Since $U_{21} = V_{01}$, incorporating (33.7)–(33.9), (36.1) in (15.1) and by using the relation (35.1), we conclude that the local truncation error associated with (15.1) may be obtained as $O(k^2h_l^2 + kh_l^3 + h_l^4)$, for arbitrary θ. Similarly, using the approximations (33.7)–(33.12), (34.1)–(34.3) in (15.2) and by the help of the relations (32.2), (35.2) and (36.2), the local truncation error associated with (15.2) is obtained as:

$$\frac{\eta(1+\eta)}{2}kh_l^2\big(\theta - \frac{1}{2}\big)U_{02} + O(k^2h_l^2 + kh_l^3 + h_l^4). \tag{37}$$

Hence, for $\theta = 1/2$, the local truncation error associated with (15.2) becomes $O(k^2h_l^2 + kh_l^3 + h_l^4)$ and thus the formula (15.1)–(15.1) is $O(k^2 + h_l^2)$ accurate.

Now, for the difference formula (16.1)–(16.2), we require high-order accuracy of the first-order partial derivatives of the solution variables at the point $(x_l, \bar{t}_j)$ defined

in (13.1)–(13.2). With the help of (34.2)–(34.3) and (10.1)–(10.14), from (13.1)–(13.2), we obtain

$$\overline{\overline{U}}_{x_l}^{j} = U_{x_l}^{j} + \theta k U_{11} + \frac{h_l^2}{6} T_3 + O(k^2 h_l + k h_l + h_l^3), \tag{38.1}$$

$$\overline{\overline{V}}_{x_l}^{j} = V_{x_l}^{j} + \theta k V_{11} + \frac{h_l^2}{6} T_4 + O(k^2 h_l + k h_l + h_l^3), \tag{38.2}$$

where

$$T_3 = (\eta + 6a_1(1+\eta))U_{30},$$
$$T_4 = (\eta + 6b_1(1+\eta)\overline{A}_l^{j})V_{30} + 6(b_1(1+\eta)\overline{A}_{x_l}^{j} + b_2)V_{20}.$$

Applying series expansion about the central grid (x_l, t_j) to (14) and incorporating (38.1)–(38.2), one obtains

$$\overline{\overline{F}}_l^{j} = F_l^{j} + kT_1 + \frac{h_l^2}{6} T_5 + O(k^2 h_l + k h_l + h_l^3), \tag{39}$$

where $T_5 = T_3 \gamma_l^{j} + T_4 \delta_l^{j}$.

Using Taylor series expansion, we first obtain

$$U_{l+1}^{j} - (1+\eta)U_l^{j} + \eta U_{l-1}^{j} = \frac{h_l^2}{12}[(\eta^2 + \eta - 1)V_{l+1}^{j} + (1+\eta)(1+3\eta+\eta^2)V_l^{j} + \eta(1+\eta-\eta^2)V_{l-1}^{j}] + O(h_l^5), \tag{40.1}$$

$$[A_l^{j} + h_l P_{1_l} A_{x_l}^{j} + h_l^2 P_{2_l} A_{xx_l}^{j}](V_{l+1}^{j} - (1+\eta)V_l^{j} + \eta V_{l-1}^{j}) + \frac{h_l^2}{12}[P_l U_{t_{l+1}}^{j} + Q_l U_{t_l}^{j} + R_l U_{t_{l-1}}^{j}]$$
$$= \frac{h_l^2}{12}[P_l F_{l+1}^{j} + Q_l F_l^{j} + R_l F_{l-1}^{j}] + O(h_l^5). \tag{40.2}$$

Using the approximations (33.4)–(33.9) in (16.1), we obtain

$$U_{l+1}^{j} - (1+\eta)U_l^{j} + \eta U_{l-1}^{j} + \frac{\theta}{2}\eta(1+\eta)kh_l^2 U_{21}$$
$$= \frac{h_l^2}{12}[(\eta^2 + \eta - 1)V_{l+1}^{j} + (1+\eta)(1+3\eta+\eta^2)V_l^{j} + \eta(1+\eta-\eta^2)V_{l-1}^{j} + 6\theta k\eta(1+\eta)V_{01}] + O(kh_l^3 + k^2 h_l^2). \tag{41}$$

Using the relation $U_{21} = V_{01}$ and (40.1) in (41), the local truncation error $\overline{T}_l^{j^{(1)}}$ associated with (16.1) may be obtained as $\overline{T}_l^{j^{(1)}} = O(k^2 h_l^2 + k h_l^3 + h_l^5)$, for arbitrary θ.

Further, invoking Taylor series expansion, we may re-write

$$[\overline{A}_l^{j} + h_l P_{1_l} \overline{A}_{x_l}^{j} + h_l^2 P_{2_l} \overline{A}_{xx_l}^{j}](\overline{V}_{l+1}^{j} - (1+\eta)\overline{V}_l^{j} + \eta \overline{V}_{l-1}^{j}) + \frac{h_l^2}{12}[P_l \overline{U}_{t_{l+1}}^{j} + Q_l \overline{U}_{t_l}^{j} + R_l \overline{U}_{t_{l-1}}^{j}]$$
$$= [A_l^{j} + h_l P_{1_l} A_{x_l}^{j} + h_l^2 P_{2_l} A_{xx_l}^{j}](V_{l+1}^{j} - (1+\eta)V_l^{j} + \eta V_{l-1}^{j}) + \frac{h_l^2}{12}[P_l U_{t_{l+1}}^{j} + Q_l U_{t_l}^{j} + R_l U_{t_{l-1}}^{j}]$$
$$+ \frac{\eta}{2}(1+\eta)kh_l^2[\theta(A_{00}V_{21} + A_{01}V_{20}) + \frac{U_{02}}{2}] + O(kh_l^3 + k^2 h_l^2). \tag{42}$$

Now using the approximations (34.2)–(34.3), (39) on the right hand side, (42) on the left hand side of (16.2) and by the help of relation (40.2), we obtain the local truncation error $\overline{T}_l^{j\,(2)}$ associated with (16.2) as:

$$\overline{T}_l^{j\,(2)} = \frac{\eta(1+\eta)}{2}kh_l^2\big(\theta-\frac{1}{2}\big)U_{02} + \frac{h_l^4}{72}[-\eta(1+\eta)P_lT_2 + Q_lT_5 - (1+\eta)R_lT_2] + O(k^2h_l^2 + kh_l^3 + h_l^5). \tag{43}$$

We observe from (43) that $\overline{T}_l^{j\,(2)}$ is of $O(k^2h_l^2 + kh_l^3 + h_l^5)$ if and only if $\theta = 1/2$ and

$$(1+\eta)(\eta P_l + R_l)T_2 = Q_lT_5,$$

from which we obtain

$$a_1 = \frac{-\eta(1+\eta+\eta^2)}{6Q_l}\left(1 + \frac{2(1-\eta)h_l\overline{A}_{xl}^j}{3\overline{A}_l^j}\right),$$

$$b_1 = \frac{-\eta(1+\eta+\eta^2)}{6\overline{A}_l^jQ_l}\left(1 + \frac{2(1-\eta)h_l\overline{A}_{xl}^j}{3\overline{A}_l^j}\right),$$

$$b_2 = \frac{\eta(1+\eta)(1+\eta+\eta^2)\overline{A}_{xl}^j}{6\overline{A}_l^jQ_l}\left(1 + \frac{2(1-\eta)h_l\overline{A}_{xl}^j}{3\overline{A}_l^j}\right).$$

Hence, for the above set of parameters, $\overline{T}_l^{j\,(2)} = O(k^2h_l^2 + kh_l^3 + h_l^5)$ and thus the difference method (16.1)–(16.2) is of $O(k^2 + kh_l + h_l^3)$ for $\theta = 1/2$.

We now consider quasi-linear problem in the coupled form given by (2.1)–(2.2) subject to the initial and boundary conditions given by (3.1)–(3.3). Here, the coefficient A is a function of not only the independent variables x and t but also of the dependent variables u and v, i.e., $A \equiv A(x,t,u,v)$. Differentiating the (2.1)–(2.2) with respect to 't' at the mesh point (x_l, t_j), we obtain:

$$U_{21} = V_{01}, \tag{44.1}$$

$$A_{00}V_{21} + [A_{01} + A_uU_{01} + A_vV_{01}]V_{20} + U_{02} = \xi_l^j + \alpha_l^jU_{01} + \beta_l^jV_{01} + \gamma_l^jU_{11} + \delta_l^jV_{11}. \tag{44.2}$$

Upon substitution of the approximations (17.1)–(17.4) and using the relations (44.1)–(44.2) in place of (32.1)–(32.2), we observe that the difference methods (15.1)–(15.2) and (16.1)–(16.2) retain their orders and hence we obtain difference methods of $O(k^2+h_l^2)$ and $O(k^2+k^2h_l+h_l^3)$, respectively, for the numerical solution of quasi-linear equations (2.1)–(2.2).

When $\eta = 1$ (uniform mesh case), that is, for $h_{l+1} = h_l = h$, $l = 1, 2, \ldots, N$, the corresponding implicit difference methods of accuracy $O(k^2 + h^2)$ and $O(k^2 + h^4)$ for the solution of differential (9.1)–(9.2) are:

$$\delta_x^2\overline{U}_l^j = h^2\overline{V}_l^j + O(k^2h^2 + h^4), \tag{45.1}$$

$$\overline{A}_l^j\delta_x^2\overline{V}_l^j + h^2\overline{U}_{tl}^j = h^2\overline{F}_l^j + O(k^2h^2 + h^4), \quad l = 1, 2, \ldots, N, \quad j = 0, 1, \ldots, J, \tag{45.2}$$

and

$$\delta_x^2 \overline{U}_l^j = \frac{h^2}{12}[\overline{V}_{l+1}^j + 10\overline{V}_l^j + \overline{V}_{l-1}^j] + O(k^2h^2 + kh^4 + h^6), \tag{46.1}$$

$$\begin{aligned}\Big[\overline{A}_l^j + \frac{h^2}{12}(\overline{A}_{xx_l}^j - \frac{2\overline{A}_{x_l}^{j^2}}{\overline{A}_l^j})\Big]\delta_x^2\overline{V}_l^j + \frac{h^2}{12}\Big[(1 - \frac{h\overline{A}_{x_l}^j}{\overline{A}_l^j})\overline{U}_{t_{l+1}}^j + 10\overline{U}_{t_l}^j + (1 + \frac{h\overline{A}_{x_l}^j}{\overline{A}_l^j})\overline{U}_{t_{l-1}}^j\Big] \\ = \frac{h^2}{12}\Big[(1 - \frac{h\overline{A}_{x_l}^j}{\overline{A}_l^j})\overline{F}_{l+1}^j + 10\overline{\overline{F}}_l^j + (1 + \frac{h\overline{A}_{x_l}^j}{\overline{A}_l^j})\overline{F}_{l-1}^j\Big] + O(k^2h^2 + kh^4 + h^6), \\ l = 1, 2, \ldots, N, \ j = 0, 1, \ldots, J,\end{aligned} \tag{46.2}$$

respectively, for $\theta = 1/2$, where $\delta_x U_l = (U_{l+1/2} - U_{l-1/2})$ is the central difference operator with respect to x-direction.

Note that for the uniform mesh case, the difference method (46.1)–(46.2) is fourth-order accurate in space for a fixed value of the mesh ratio parameter $\lambda = k/h^2$.

4 Stability analysis and difference schemes for a singular equation

We shall discuss the stability for the uniform mesh case. Consider the following 1D unsteady linear biharmonic problem of the form

$$\frac{\partial^4 u}{\partial x^4} + \frac{\partial u}{\partial t} = f(x,t), \quad (x,t) \in \Omega, \tag{47}$$

subject to the initial and boundary conditions (3.1)–(3.2). Applying the difference methods (45.1)–(45.2) and (46.1)–(46.2) to the differential equation (47), we obtain the matrix equation

$$Q\, w^{j+1} = (-Q + R)\, w^j + l, \tag{48}$$

where

$$Q = \begin{bmatrix} Q_1 & -h^2 Q_2 \\ Q_2 & \frac{\lambda}{2} Q_1 \end{bmatrix}, \quad R = \begin{bmatrix} 0 & 0 \\ 2Q_2 & 0 \end{bmatrix}, \quad w = \begin{bmatrix} u \\ v \end{bmatrix}, \quad l = \begin{bmatrix} l_1 \\ l_2 \end{bmatrix}.$$

The matrices Q and R are $2N \times 2N$ block tri-diagonal while w and l are column vectors of order $2N$. Equation (48) is the matrix form of the finite difference equation relating the solution values along the $(j+1)$th and jth time levels in which Q and R are the coefficient matrices, w is the solution vector, and l denotes the column vector of known boundary values and right hand side function values of (47).

The submatrices for method (45.1)–(45.2) are given by $Q_1 = [1, -2, 1]$, $Q_2 = [0, 1, 0]$ while the submatrices for method (46.1)–(46.2) are given by $Q_1 = 12[1, -2, 1]$, $Q_2 = [1, 10, 1]$ where

$$[a, b, c] = \begin{bmatrix} b & c & 0 & \cdots & 0 \\ a & b & c & & \vdots \\ 0 & \ddots & \ddots & \ddots & 0 \\ \vdots & & a & b & c \\ 0 & \cdots & 0 & a & b \end{bmatrix}$$

is the $N \times N$ tri-diagonal matrix having eigenvalues $b + 2\sqrt{a\,c}\cos(2\phi)$, $2\phi = (s\pi)/(N+1)$, $s = 1(1)N$; $u = (u_1, u_2, \ldots, u_N)^T$, $v = (v_1, v_2, \ldots, v_N)^T$ are solution vectors and l_1, l_2 are column vectors of order N consisting of homogenous functions, initial and boundary values of the block system (48). Note that u_0, u_{N+1} and v_0, v_{N+1} are known from the imposed boundary conditions and $\lambda = k/h^2$ is the mesh ratio parameter for the uniform mesh (for $\eta = 1$, that is, for $h_{l+1} = h_l = h$). We see that l_1 is the zero column vector of order N for both the difference methods (45.1)–(45.2) and (46.1)–(46.2). For the difference method (45.1)–(45.2),

$$l_2 = \begin{bmatrix} kf(x_1, \bar{t}_j) - \frac{\lambda}{2}\left(v_0^{j+1} + v_0^j\right) \\ kf(x_2, \bar{t}_j) \\ \cdots \\ \cdots \\ kf(x_{N-1}, \bar{t}_j) \\ kf(x_N, \bar{t}_j) - \frac{\lambda}{2}\left(v_{N+1}^{j+1} + v_{N+1}^j\right) \end{bmatrix},$$

while for the difference method (46.1)–(46.2),

$$l_2 = \begin{bmatrix} k\left(f(x_2, \bar{t}_j) + 10f(x_1, \bar{t}_j) + f(x_0, \bar{t}_j)\right) - \left(u_0^{j+1} + u_0^j\right) - 6\lambda\left(v_0^{j+1} + v_0^j\right) \\ k\left(f(x_3, \bar{t}_j) + 10f(x_2, \bar{t}_j) + f(x_1, \bar{t}_j)\right) \\ \cdots \\ \cdots \\ k\left(f(x_N, \bar{t}_j) + 10f(x_{N-1}, \bar{t}_j) + f(x_{N-2}, \bar{t}_j)\right) \\ k\left(f(x_{N+1}, \bar{t}_j) + 10f(x_N, \bar{t}_j) + f(x_{N-1}, \bar{t}_j)\right) - \left(u_{N+1}^{j+1} + u_{N+1}^j\right) - 6\lambda\left(v_{N+1}^{j+1} + v_{N+1}^j\right) \end{bmatrix}.$$

For discussing the stability of differential equation (47), we consider the homogenous part of the difference scheme (48), which may be written as

$$w^{j+1} = (-I + Q^{-1} R)\, w^j. \tag{49}$$

We denote $\varepsilon^j = w^j - W^j$ as the error vector at the jth iterate (in the absence of round-off errors), where

$$W^j = \begin{bmatrix} U \\ V \end{bmatrix}^j,$$

U and V being exact solution vectors. We may write the error equation as:

$$\varepsilon^{j+1} = H\varepsilon^j,$$

where the amplification matrix H is given by $H = -I + Q^{-1} R$. The eigenvalues ξ of matrix Q for method (45.1)–(45.2) satisfies the characteristic equation

$$\det \begin{bmatrix} -4\sin^2\phi - \xi & -h^2 \\ 1 & -2\lambda\sin^2\phi - \xi \end{bmatrix} = 0, \tag{50}$$

which on simplification gives

$$\xi^2 + 2\sin^2\phi(\lambda + 2)\xi + 8\lambda\sin^4\phi + h^2 = 0. \tag{51}$$

The eigenvalues ξ of matrix Q for method (46.1)–(46.2) satisfies the characteristic equation

$$\det \begin{bmatrix} -48\sin^2\phi - \xi & -h^2(12 - 4\sin^2\phi) \\ 12 - 4\sin^2\phi & -24\lambda\sin^2\phi - \xi \end{bmatrix} = 0, \tag{52}$$

which gives

$$\xi^2 + 24\sin^2\phi(\lambda+2)\xi + h^2(12 - 4\sin^2\phi)^2 + 1152\lambda\sin^4\phi = 0. \tag{53}$$

Further, 0 is the only eigenvalue of matrix R, and since Q^{-1} and R commute each other, hence eigenvalue η of the amplification matrix H for methods (45.1)–(45.2) and (46.1)–(46.2) is given by $\eta = -1$. Since $|\eta| = 1$ for all variable angle ϕ and $\lambda > 0$, hence the methods are stable for all values of the mesh ratio parameter λ.

Next, we aim to discuss the stable difference schemes for a class of 1D unsteady linear biharmonic equations with singular coefficients and ensure that the methods developed retain their order and accuracy for such equations.

Let us consider a class of 1D unsteady linear singular biharmonic problem of the form:

$$\nabla^4 u + \frac{\partial^2 u}{\partial t^2} \equiv \left(\frac{\partial^2}{\partial r^2} + \frac{\alpha}{r}\frac{\partial}{\partial r}\right)^2 u + \frac{\partial u}{\partial t} = g(r,t),$$

where $(r,t) \in \Lambda \equiv \{(r,t) | \, 0 < r < 1, \ t > 0\}$, or equivalently,

$$\frac{\partial^4 u}{\partial r^4} + \frac{\partial u}{\partial t} = B(r)\frac{\partial^3 u}{\partial r^3} + C(r)\frac{\partial^2 u}{\partial r^2} + D(r)\frac{\partial u}{\partial r} + g(r,t), \quad (r,t) \in \Lambda, \tag{54}$$

where

$$B(r) = \frac{-2\alpha}{r}, \quad C(r) = \frac{\alpha(2-\alpha)}{r^2}, \quad D(r) = \frac{\alpha(\alpha-2)}{r^3},$$

subject to the following initial and boundary conditions

$$u(r,0) = u_0(r), \quad 0 \le r \le 1, \tag{55.1}$$

$$u(0,t) = g_0(t), \quad u(0,t) = g_1(t), \quad t > 0, \tag{55.2}$$

$$u_{rr}(1,t) = h_0(t), \quad u_{rr}(1,t) = h_1(t), \quad t > 0. \tag{55.3}$$

For $\alpha = 1$ and 2,

$$\nabla^2 \equiv \frac{\partial^2}{\partial r^2} + \frac{\alpha}{r}\frac{\partial}{\partial r}$$

represents one-space dimensional Laplacian operator in cylindrical and spherical coordinates, respectively, so for $\alpha = 1$ and 2, (54) is the 1D unsteady biharmonic equation in cylindrical and spherical coordinates, respectively. Using the second-order central differences, the numerical solution of the above equation can be obtained making use of five grid points in r-direction and discretizing the boundary conditions. But so far, no two-level difference method on a variable mesh of $O(k^2 + kh_l + h_l^3)$ using only three spatial grid points and without discretizing the boundary conditions is known for the singular equation (54). The finite difference methods discussed here requires no fictitious points for incorporating the boundary conditions. It is difficult to determine the numerical solution of (54) as the solution deteriorates in the vicinity of the singularity $r = 0$. We overcome this difficulty by

modifying our methods in such a manner that the order and accuracy of the solution is retained everywhere including the region in the vicinity of the singularity $r = 0$.

Applying the difference method (15.1)–(15.2) of $O(k^2 + h_l^2)$, we obtain

$$\overline{u}_{l+1}^j - (1+\eta)\overline{u}_l^j + \eta\overline{u}_{l-1}^j = \frac{h_l^2}{6}[(\eta-1)\overline{v}_{l+1}^j + (1+\eta)(1+\eta+\eta^2)\overline{v}_l^j - \eta^2(\eta-1)\overline{v}_{l-1}^j], \tag{56.1}$$

$$\begin{aligned}
&\overline{v}_{l+1}^j - (1+\eta)\overline{v}_l^j + \eta\overline{v}_{l-1}^j + \frac{h_l^2}{6}[(\eta-1)\overline{u}_{r_{l+1}}^j + (1+\eta+\eta^2)(1+\eta)\overline{u}_{r_l}^j - \eta^2(\eta-1)\overline{u}_{r_{l-1}}^j] \\
&= \frac{h_l^2}{6}\big[(\eta-1)(B_{l+1}\overline{v}_{r_{l+1}}^j + C_{l+1}\overline{v}_{l+1}^j + D_{l+1}\overline{u}_{r_{l+1}}^j + \overline{g}_{l+1}^j) \\
&\quad +(1+\eta+\eta^2)(1+\eta)(B_l\overline{v}_{r_l}^j + C_l\overline{v}_l^j + D_l\overline{u}_{r_l}^j + \overline{g}_l^j) \\
&\quad -\eta^2(\eta-1)(B_{l-1}\overline{v}_{r_{l-1}}^j + C_{l-1}\overline{v}_{l-1}^j + D_{l-1}\overline{u}_{r_{l-1}}^j + \overline{g}_{l-1}^j)\big], \\
&\qquad\qquad l = 1, 2, \ldots, N,\ \ j = 0, 1, \ldots, J,\quad \eta \neq 1,
\end{aligned} \tag{56.2}$$

where for $p = 0, \pm 1$: $B_{l+p} = B(r_{l+p})$, $C_{l+p} = C(r_{l+p})$, $D_{l+p} = D(r_{l+p})$, $\overline{g}_{l+p}^j = g(r_{l+p}, \overline{t}_j)$.

The above scheme fails to determine the solution at $l = 1$, in the vicinity of the singularity. We overcome this difficulty by modifying the scheme (56.1)–(56.2) in such a way that the solutions retain their order and accuracy everywhere including the vicinity of the singularity r = 0. We need the following approximations:

$$B_{l+1} = B_{00} + \eta h_l B_{10} + O(h_l^2) \equiv B_1^* + O(h_l^2), \tag{57.1}$$

$$B_{l-1} = B_{00} - h_l B_{10} + O(h_l^2), \equiv B_2^* + O(h_l^2) \tag{57.2}$$

$$C_{l+1} = C_{00} + \eta h_l C_{10} + O(h_l^2) \equiv C_1^* + O(h_l^2), \tag{57.3}$$

$$C_{l-1} = C_{00} - h_l C_{10} + O(h_l^2) \equiv C_2^* + O(h_l^2), \tag{57.4}$$

$$D_{l+1} = D_{00} + \eta h_l D_{10} + O(h_l^2) \equiv D_1^* + O(h_l^2), \tag{57.5}$$

$$D_{l-1} = D_{00} - h_l D_{10} + O(h_l^2) \equiv D_2^* + O(h_l^2), \tag{57.6}$$

$$\overline{g}_{l+1}^j = \overline{g}_l^j + \eta h_l \overline{g}_{r_l}^j + O(h_l^2) \equiv G_1^* + O(h_l^2), \tag{57.7}$$

$$\overline{g}_{l-1}^j = \overline{g}_l^j - h_l \overline{g}_{r_l}^j + O(h_l^2) \equiv G_2^* + O(h_l^2). \tag{57.8}$$

where

$$B_1^* = B_{00} + \eta h_l B_{10}, \quad B_2^* = B_{00} - h_l B_{10}, \text{ etc.}$$

Using the approximations (57.1)–(57.8) in the scheme (56.1)–(56.2) and neglecting high order terms, we get

$$\overline{u}_{l+1}^j - (1+\eta)\overline{u}_l^j + \eta\overline{u}_{l-1}^j = \frac{h_l^2}{6}[(\eta-1)\overline{v}_{l+1}^j + (1+\eta)(1+\eta+\eta^2)\overline{v}_l^j - \eta^2(\eta-1)\overline{v}_{l-1}^j], \tag{58.1}$$

$$\begin{aligned}
&\overline{v}_{l+1}^j - (1+\eta)\overline{v}_l^j + \eta\overline{v}_{l-1}^j + \frac{h_l^2}{6}[(\eta-1)\overline{u}_{r_{l+1}}^j + (1+\eta+\eta^2)(1+\eta)\overline{u}_{r_l}^j - \eta^2(\eta-1)\overline{u}_{r_{l-1}}^j] \\
&= \frac{h_l^2}{6}\big[(\eta-1)(B_1^*\overline{v}_{r_{l+1}}^j + C_1^*\overline{v}_{l+1}^j + D_1^*\overline{u}_{r_{l+1}}^j + G_1^* \\
&\quad +(1+\eta+\eta^2)(1+\eta)(B_{00}\overline{v}_{r_l}^j + C_{00}\overline{v}_l^j + D_{00}\overline{u}_{r_l}^j + g_{00}) \\
&\quad -\eta^2(\eta-1)(B_2^*\overline{v}_{r_{l-1}}^j + C_2^*\overline{v}_{l-1}^j + D_2^*\overline{u}_{r_{l-1}}^j + G_2^*)\big], \\
&\qquad\qquad l = 1, 2, \ldots, N,\ \ j = 0, 1, \ldots, J,\quad \eta \neq 1,
\end{aligned} \tag{58.2}$$

which is a valid difference scheme of $O(k^2+h_l^2)$ in the region $[0<r<1]\times[t>0]$.

The proposed difference method (16.1)–(16.2) of $O(k^2+kh_l+h_l^3)$ when applied to the singular equation (54) results in the following difference scheme:

$$\begin{aligned}\overline{u}_{l+1}^j-(1+\eta)\overline{u}_l^j+\eta\overline{u}_{l-1}^j&=\frac{h_l^2}{12}\big[(\eta^2+\eta-1)\overline{v}_{l+1}^j+(1+\eta)(1+3\eta+\eta^2)\overline{v}_l^j\\&\qquad+\eta(1+\eta-\eta^2)\overline{v}_{l-1}^j\big],\end{aligned}\tag{59.1}$$

$$\begin{aligned}&\overline{v}_{l+1}^j-(1+\eta)\overline{v}_l^j+\eta\overline{v}_{l-1}^j+\frac{h_l^2}{12}[(\eta^2+\eta-1-p_0)\overline{u}_{t_{l+1}}^j+(1+\eta)(1+3\eta+\eta^2)\overline{u}_{t_l}^j\\&+(\eta(1+\eta-\eta^2)+p_0)\overline{u}_{t_{l-1}}^j]\\&=\frac{h_l^2}{12}\Big[\big(\eta^2+\eta-1-p_0\big)\big(B_{l+1}\overline{v}_{r_{l+1}}^j+C_{l+1}\overline{v}_{l+1}^j+D_{l+1}\overline{u}_{r_{l+1}}^j+\overline{g}_{l+1}^j\big)\\&\qquad+(1+\eta)(1+3\eta+\eta^2)\big(B_l\overline{v}_{r_l}^j+C_l\overline{v}_l^j+D_l\overline{u}_{r_l}^j+\overline{g}_l^j\big)-q_0(\overline{v}_{l+1}^j-\overline{v}_{l-1}^j)\\&\qquad+\big(\eta(1+\eta-\eta^2)+p_0\big)\big(B_{l-1}\overline{v}_{r_{l-1}}^j+C_{l-1}\overline{v}_{l-1}^j+D_{l-1}\overline{u}_{r_{l-1}}^j+\overline{g}_{l-1}^j\big)\Big],\\&\qquad l=1,2,\ldots,N,\ \ j=0,1,\ldots,J,\end{aligned}\tag{59.2}$$

where $p_0=(\eta(1+\eta+\eta^2)h_lB_l)/6,\ q_0=(\eta(1+\eta+\eta^2)h_lD_l)/6$.

Although the difference scheme (59.1)–(59.2) is of $O(k^2+kh_l+h_l^3)$, it contains the terms $B_{l-1},\ C_{l-1},\ D_{l-1},\ \overline{g}_{l-1}^j$, all of which involve the term $1/r_{l-1}$ giving rise to singularity at $l=1$ since $r_0=0$. It is for this reason that the proposed method is not directly applicable to singular equations in the region $0<r<1$, i.e., in the vicinity of singularity. We overcome this difficulty by modifying the method (59.2) in such a manner that the order and accuracy of the solution is retained everywhere in the region $[0<r<1]\times[t>0]$, even in the vicinity of the singularity $r=0$.

In order to get a valid difference scheme of $O(k^2+kh_l+h_l^3)$ on a variable mesh, we require the following approximations:

$$B_{l+1}=B_{00}+\eta h_lB_{10}+\frac{\eta^2h_l^2}{2}B_{20}+O(h_l^3)\equiv B_1+O(h_l^3),\tag{60.1}$$

$$B_{l-1}=B_{00}-h_lB_{10}+\frac{h_l^2}{2}B_{20}-O(h_l^3)\equiv B_2-O(h_l^3),\tag{60.2}$$

$$C_{l+1}=C_{00}+\eta h_lC_{10}+\frac{\eta^2h_l^2}{2}C_{20}+O(h_l^3)\equiv C_1+O(h_l^3),\tag{60.3}$$

$$C_{l-1}=C_{00}-h_lC_{10}+\frac{h_l^2}{2}C_{20}-O(h_l^3)\equiv C_2-O(h_l^3),\tag{60.4}$$

$$D_{l+1}=D_{00}+\eta h_lD_{10}+\frac{\eta^2h_l^2}{2}D_{20}+O(h_l^3)\equiv D_1+O(h_l^3),\tag{60.5}$$

$$D_{l-1}=D_{00}-h_lD_{10}+\frac{h_l^2}{2}D_{20}-O(h_l^3)\equiv D_2-O(h_l^3),\tag{60.6}$$

$$\overline{g}_{l+1}^j=\overline{g}_l^j+\eta h_l\overline{g}_{r_l}^j+\frac{\eta^2h_l^2}{2}\overline{g}_{rr_l}^j+O(h_l^3)\equiv G_1+O(h_l^3),\tag{60.7}$$

$$\overline{g}_{l-1}^j=\overline{g}_l^j-h_l\overline{g}_{r_l}^j+\frac{h_l^2}{2}\overline{g}_{rr_l}^j-O(h_l^3)\equiv G_2-O(h_l^3).\tag{60.8}$$

where

$$B_1 = B_{00} + \eta h_l B_{10} + \frac{\eta^2 h_l^2}{2} B_{20}, \quad B_2 = B_{00} - h_l B_{10} + \frac{h_l^2}{2} B_{20}, \text{ etc.}$$

and $\overline{g}^j_{r_l} = g_r(r_l, \bar{t}_j)$, $\overline{g}^j_{rr_l} = g_{rr}(r_l, \bar{t}_j)$. Using the approximations (60.1)–(60.8) in the difference scheme (59.1)–(59.2) and neglecting the higher-order terms, we obtain

$$\overline{u}^j_{l+1} - (1+\eta)\overline{u}^j_l + \eta \overline{u}^j_{l-1} = \frac{h_l^2}{12}\big[(\eta^2+\eta-1)\overline{v}^j_{l+1} + (1+\eta)(1+3\eta+\eta^2)\overline{v}^j_l + \eta(1+\eta-\eta^2)\overline{v}^j_{l-1}\big], \tag{61.1}$$

$$\begin{aligned}
&\overline{v}^j_{l+1} - (1+\eta)\overline{v}^j_l + \eta\overline{v}^j_{l-1} + \frac{h_l^2}{12}[(\eta^2+\eta-1-p_0)\overline{u}^j_{l_{l+1}} + (1+\eta)(1+3\eta+\eta^2)\overline{u}^j_{l_l} \\
&+(\eta(1+\eta-\eta^2)+p_0)\overline{u}^j_{l_{l-1}}] \\
&= \frac{h_l^2}{12}\Big[\big(\eta^2+\eta-1-p_0\big)\big(B_1\overline{v}^j_{r_{l+1}} + C_1\overline{v}^j_{l+1} + D_1\overline{u}^j_{r_{l+1}} + G_1\big) \\
&\qquad +(1+\eta)(1+3\eta+\eta^2)\big(B_{00}\overline{v}^j_{r_l} + C_{00}\overline{v}^j_l + D_{00}\overline{u}^j_{r_l} + g_{00}\big) - q_0(\overline{v}^j_{l+1} - \overline{v}^j_{l-1}) \\
&\qquad +\big(\eta(1+\eta-\eta^2)+p_0\big)\big(B_2\overline{v}^j_{r_{l-1}} + C_2\overline{v}^j_{l-1} + D_2\overline{u}^j_{r_{l-1}} + G_2\big)\Big], \\
&\qquad\qquad l = 1, 2, \ldots, N, \ \ j = 0, 1, \ldots, J.
\end{aligned} \tag{61.2}$$

Note that the difference scheme (61.1)–(61.2) is a two-level implicit scheme of $O(k^2 + kh_l + h_l^3)$ which does not involve the term $1/r_{l-1}$, hence can be very easily solved for $l = 1, 2, \ldots, N$ in the region $[0 < r < 1] \times [t > 0]$. The resulting system of tri-diagonal matrices can be solved using block iterative methods (see Kelly [12]).

5 Numerical illustrations

In this section, we implement the proposed difference methods over a collection of linear and nonlinear problems having physical importance. The exact solutions of the problems are provided in each case. The right hand side homogenous function, initial and boundary conditions correspond to the data from the exact solution. Whenever the differential equation (1) is nonlinear or quasi-linear, then the proposed difference formulas form a coupled nonlinear block system. We have used iterative methods for solving the coupled system of equations at each mesh point. If the differential (1) is linear, then the resulting system is solved by block Gauss-Seidel iteration method whereas the nonlinear systems are solved using Newton's nonlinear block Gauss-Seidel iteration method (see Kelly [12], Saad [23] and Hageman and Young [9]) and in each case the iterations are terminated once the absolute error tolerance $\leq 10^{-10}$ is achieved.

Table 1 The maximum absolute errors for Example 1 at $t = 1.0,\ \eta = 0.94$ (variable mesh)

$N+1$		$O(k^2 + kh_l + h_l^3)$-method (16.1)–(16.2)		$O(k^2 + h_l^2)$-method (15.1)–(15.2)	
		$\alpha = 1$	$\alpha = 2$	$\alpha = 1$	$\alpha = 2$
8	u	2.4607(−04)	1.1207(−03)	1.5739(−03)	3.3012(−03)
	u_{rr}	4.9997(−03)	2.4233(−02)	5.7765(−02)	7.5181(−02)
16	u	2.8482(−05)	1.6480(−04)	3.2114(−04)	6.9671(−04)
	u_{rr}	1.2191(−03)	6.8188(−03)	1.5140(−02)	1.9540(−02)
32	u	6.1012(−06)	3.9682(−05)	6.0043(−05)	1.4908(−04)
	u_{rr}	3.4265(−04)	2.6947(−03)	5.3493(−03)	9.7255(−03)

For uniform mesh, $\eta = 1$ and for variable mesh, the interval $[a, b]$ in x-direction is divided into $N+1$ parts with $a = x_0 < x_1 < \ldots < x_N < x_{N+1} = b,$ where $h_l = x_l - x_{l-1},\ l = 1, 2, \ldots, N+1$ and $\eta = (h_{l+1}/h_l) > 0,\ l = 1, 2, \ldots, N$. Since

$$\begin{aligned} b - a &= x_{N+1} - x_0 = (x_{N+1} - x_N) + (x_N - x_{N-1}) + \cdots + (x_1 - x_0) \\ &= h_{N+1} + h_N + \cdots + h_1 \\ &= h_1(1 + \eta + \eta^2 + \cdots + \eta^N), \end{aligned}$$

which gives the value of the first step length in x-direction as

$$h_1 = \frac{(b-a)(1-\eta)}{1-\eta^{N+1}}, \quad \eta \neq 1. \tag{62}$$

Thus, having prescribed the value of η and total number of mesh points in the x-direction as $N+2$ with $N+1$ subintervals, we can calculate h_1 from the above relation and the remaining mesh lengths in x-direction are known by $h_{l+1} = \eta h_l,\ l =$

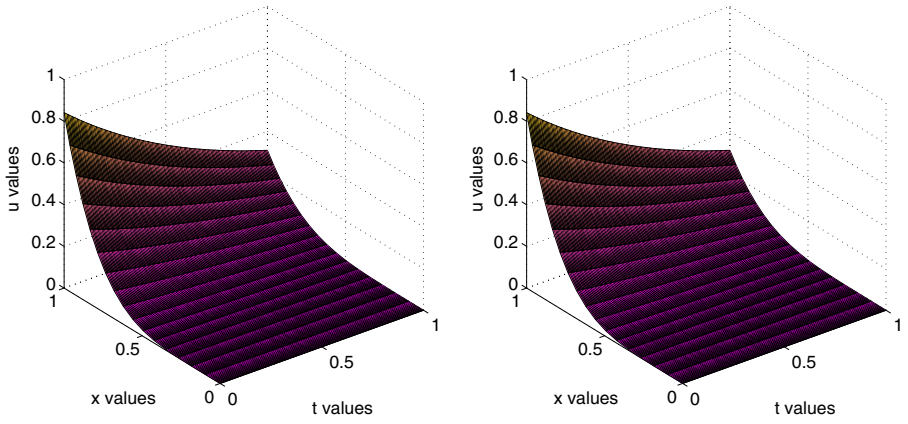

(a) Numerical Solution (b) Exact Solution

Fig. 1 Example 1: The graph of numerical and exact solution for $\alpha = 1$, $\eta = 0.94$ and $N+1 = 16$ at $t = 1$ with $\min_{1 \le l \le N+1} h_l = 0.0377$ and $\max_{1 \le l \le N+1} h_l = 0.0955$

Table 2 The maximum absolute errors for Example 2 at $t = 1.0$, $\eta = 1.08$ (variable mesh)

$N+1$		$O(k^2 + kh_l + h_l^3)$-method (16.1)–(16.2)			$O(k^2 + h_l^2)$-method (15.1)–(15.2)		
		$\alpha = 10$	$\alpha = 20$	$\alpha = 40$	$\alpha = 10$	$\alpha = 20$	$\alpha = 40$
8	u	9.6855(−05)	7.7079(−05)	6.2282(−05)	7.5101(−03)	6.1608(−03)	4.8730(−03)
	u_{xx}	7.4891(−03)	7.2465(−03)	6.8882(−03)	1.6228(−01)	1.4935(−01)	1.3764(−01)
16	u	2.1191(−05)	1.7910(−05)	1.4694(−05)	2.3124(−03)	1.9097(−03)	1.5264(−03)
	u_{xx}	1.4068(−03)	1.3918(−03)	1.3753(−03)	5.5398(−02)	5.2045(−02)	4.8772(−02)
32	u	8.1361(−06)	6.9275(−06)	5.7831(−06)	1.0341(−03)	8.6087(−04)	6.9501(−04)
	u_{xx}	6.5429(−04)	6.5008(−04)	6.4540(−04)	2.8087(−02)	2.6594(−02)	2.5095(−02)

$1, 2, \ldots, N$. Hence, each grid point (x_l, t_j) of the mesh is determined. Throughout our computation (wherever not specified), we have used the time step $k = 1.6/(N+1)^2$ for finding the solution at $t = 1$.

Example 1 (*1D unsteady singular biharmonic equation*) We solve numerically the differential equation (54) whose exact solution is $u = e^{-t} r^4 \sin r$. The maximum absolute error is considered for testing the accuracy of the methods defined as

$$\text{MAE} = \max_{1 \le l \le N} |u(x_l, t) - u^*(x_l, t)|,$$

where $u(x_l, t)$, $u^*(x_l, t)$ denotes the numerical and exact solution, respectively. The maximum absolute errors in u and u_{rr} with $\eta = 0.94$ are listed in Table 1 at $t = 1$ for $\alpha = 1, 2$. Figure 1 gives a comparison of the plots of the exact and numerical solutions using method (61.1)–(61.2).

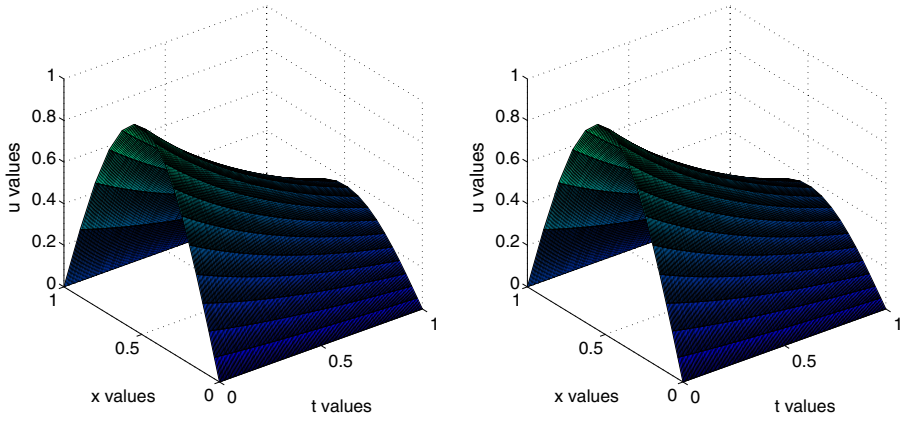

(a) Numerical Solution (b) Exact Solution

Fig. 2 Example 2: The graph of numerical and exact solution for $\alpha = 20$, $\eta = 1.08$ and $N + 1 = 16$ at $t = 1$ with $\min_{1 \le l \le N+1} h_l = 0.0330$ and $\max_{1 \le l \le N+1} h_l = 0.1046$

Table 3 The absolute errors in u for the generalized fourth-order KdV equation (4), Example 3 with $p = 4,\ c = 0.05,\ K = 0.1$ and $A = 0.2$ (uniform mesh)

t		x				
		0.1	0.2	0.3	0.4	0.5
0.1	Method (46.1)–(46.2)	9.9124(−07)	1.8988(−06)	2.6425(−06)	3.1510(−06)	3.3679(−06)
	Method discussed in [11]	5.5554(−06)	1.1081(−05)	1.6575(−05)	2.2040(−05)	2.7475(−05)
0.2	Method (46.1)–(46.2)	8.8986(−07)	1.7064(−06)	2.3785(−06)	2.8423(−06)	3.0464(−06)
	Method discussed in [11]	5.7876(-06)	1.1546(−05)	1.7275(−05)	2.2976(−05)	2.8647(−05)
0.3	Method (46.1)–(46.2)	7.9102(−07)	1.5186(−06)	2.1198(−06)	2.5377(−06)	2.7259(−06)
	Method discussed in [11]	6.0145(−06)	1.2001(−05)	1.7959(−05)	2.3890(−05)	2.9792(−05)
0.4	Method (46.1)–(46.2)	6.9173(−07)	1.3302(−06)	1.8610(−06)	2.2336(−06)	2.4059(−06)
	Method discussed in [11]	6.2362(−06)	1.2446(−05)	1.8628(−05)	2.4784(−05)	2.7475(−05)
0.5	Method (46.1)–(46.2)	5.9199(−07)	1.1413(−06)	1.6019(−06)	1.9295(−06)	2.0862(−06)
	Method discussed in [11]	6.4530(−06)	1.2880(−05)	1.9282(−05)	2.5658(−05)	3.2008(−05)

Example 2 (*1D unsteady quasi-linear biharmonic equation*)

$$\left(1+u^2\right)\frac{\partial^4 u}{\partial x^4}+\frac{\partial u}{\partial t}=\alpha u u_{xx}+f(x,t),\quad 0<x<1,\quad t>0, \tag{63}$$

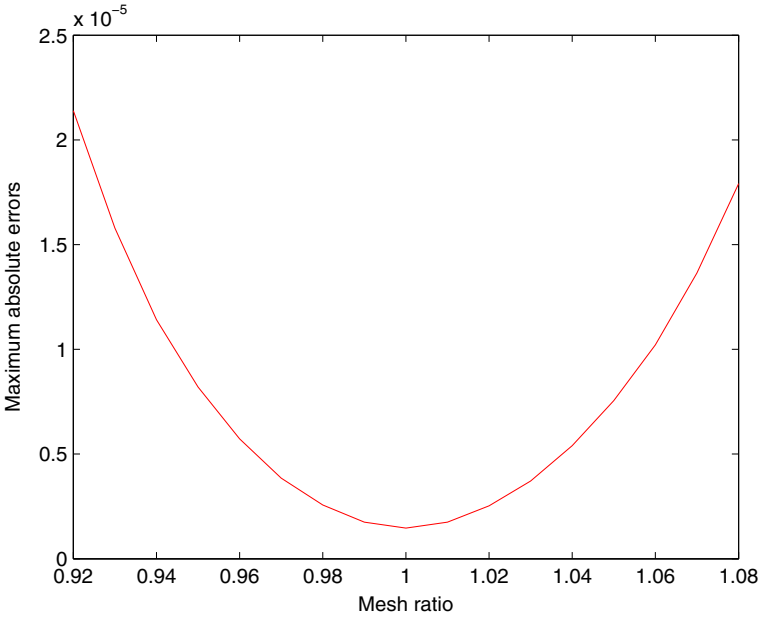

Fig. 3 Example 2: Error plot with varying mesh ratio at $t = 1$ ($\alpha = 20$ and $N + 1 = 16$ in Example 2)

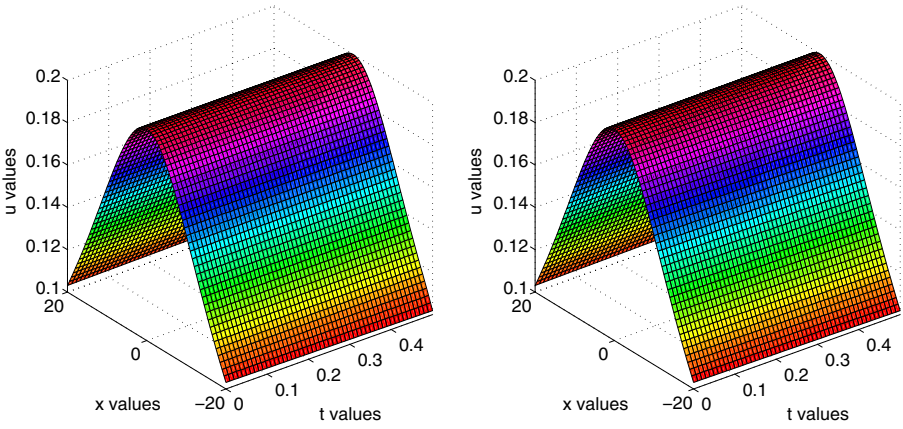

(a) Numerical Solution (b) Exact Solution

Fig. 4 Example 3: The graph of numerical and exact solution of homogenous generalized fourth-order KdV equation (4) for $p = 4,\ c = 0.05,\ K = 0.1, A = 0.2$ at $t = 0.5$ and for $-20 < x < 20$

where

$$f(x,t) = \left[\pi^4\left(1 + e^{-2t}\sin^2(\pi x)\right) - 1 + \alpha\pi^2 e^{-t}\sin(\pi x)\right]e^{-t}\sin(\pi x).$$

The exact solution is $u(x,t) = e^{-t}\sin(\pi x)$. The quasi-linear equation (63) in which the coefficient $A(x,t,u,u_{xx}) \equiv 1 + u^2$ is solved using the approximations (17.1)–(17.2) in the difference formula (16.1)–(16.2). The maximum absolute errors in u and u_{xx} with $\eta = 1.08$ are listed in Table 2 at $t = 1$ for various values of α. Figure 2 gives a comparison of the plots of the exact and numerical solutions. In order to illustrate the effect in the accuracy of the scheme (16.1)–(16.2) with varying mesh ratio, the maximum absolute errors are plotted at $t = 1$ in Fig. 3 for $\alpha = 20$ and $N + 1 = 16$ with mesh ratio varying from 0.92 to 1.08. It is observed from Fig. 3 that the error is minimum for $\eta = 1$ (uniform mesh) and fourth-order accurate results are obtained while the error increases as the mesh ratio varies from unity.

Table 4 The maximum absolute errors for non-homogenous fourth-order nonlinear KdV equation (64), Example 4 at $t = 1.0,\ \eta = 0.92$ for various values of p (variable mesh)

$N+1$		$O(k^2 + kh_l + h_l^3)$-method (16.1)–(16.2)			$O(k^2 + h_l^2)$-method (15.1)–(15.2)		
		$p = 4$	$p = 6$	$p = 8$	$p = 4$	$p = 6$	$p = 8$
8	u	1.1291(−05)	3.1582(−05)	1.0103(−04)	3.1935(−04)	4.1000(−04)	2.9101(−03)
	u_{xx}	4.1053(−04)	2.2876(−03)	8.4276(−03)	1.8103(−02)	7.0936(−02)	1.6960(−01)
16	u	1.5093(−06)	5.1481(−06)	2.4821(−05)	1.1170(−04)	2.1159(−04)	1.0707(−03)
	u_{xx}	1.4344(−04)	1.0158(−03)	3.9896(−03)	1.0767(−02)	4.6772(−02)	1.2559(−01)
32	u	5.0662(−07)	1.8546(−06)	1.0592(−05)	6.0383(−05)	1.2508(−04)	5.9424(−04)
	u_{xx}	8.2770(−05)	6.0844(−04)	2.4633(−03)	7.5403(−03)	3.4048(−02)	9.5377(−02)

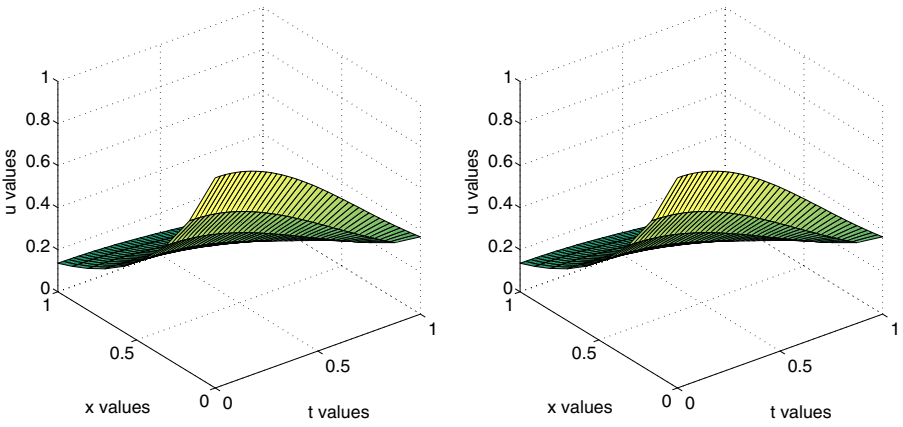

(a) Numerical Solution (b) Exact Solution

Fig. 5 Example 4: The graph of numerical and exact solution of non-homogenous generalized fourth-order KdV equation (64) for $p = 4$, $\eta = 0.92$ and $N + 1 = 8$ at $t = 1$ with $\min_{1\le l\le N+1} h_l = 0.0917$ and $\max_{1\le l\le N+1} h_l = 0.1643$

Example 3 (*Generalized fourth-order KdV equation*) The generalized fourth-order KdV equation (4) admits single-soliton solutions as $u(x,t) = A[\text{sech}^2(Kx - ct)]^{1/p}$ where A, K and c are constants (see [11]). We compute the above traveling wave solution of (4) by using the difference method (45.1)–(45.2) for uniform mesh and compare our results with the Adomian decomposition method proposed by Kaya [11]. We take the same constants as in [11]: $p = 4$, $c = 0.05$, $K = 0.1$ and $A = 0.2$. The absolute errors are tabulated in Table 3 at various time levels $t = 0.1, 0.2, 0.3, 0.4$ and 0.5. The 3D graphs of numerical and analytical solutions are plotted in Fig. 4 for $p = 4,\ c = 0.05,\ K = 0.1, A = 0.2$ and for $-20 < x < 20$.

Table 5 Comparison of global relative error in u for the KS equation (6), Example 5 with $\alpha = 1$ and $\gamma = 1$ at different times

t	$O(k^2 + h^4)$-method	Method discussed	Method discussed
	(46.1)–(46.2)	in [20]	in [17]
1	6.0297(−05)	3.8173(−04)	6.7923(−04)
2	9.9303(−05)	5.5114(−04)	1.1503(−03)
3	1.3064(−04)	7.0398(−04)	1.5941(−03)
4	1.6060(−04)	8.6366(−04)	2.0075(−03)

Example 4 (*Non-homogenous fourth-order non-linear KdV equation*) We conducted an accuracy test using variable mesh difference method (16.1)–(16.2) for the non-homogenous fourth-order KdV equation (see [21]):

$$\frac{\partial^4 u}{\partial x^4} + \frac{\partial u}{\partial t} + (p+1)u^p u_x = f(x,t), \quad p > 2, \quad 0 < x < 1, \quad t > 0, \tag{64}$$

where

$$f(x,t) = \left[\frac{p^4}{16} - 2t - \frac{p}{2}(p+1)e^{-p\left(\frac{px}{2}+t^2\right)}\right]e^{-\left(\frac{px}{2}+t^2\right)}.$$

The exact solution is given by $u(x,t) = e^{-(\frac{px}{2}+t^2)}$. The maximum absolute errors in u and u_{xx} with $\eta = 0.92$ are listed in Table 4 at $t = 1$ for $p = 4$, 6 and 8. Figure 5 gives a comparison of the plots of the exact and numerical solutions using method (16.1)–(16.2) for $p = 4$.

Example 5 (*Kuramoto-Sivashinsky equation with* $\alpha = 1$ *and* $\gamma = 1$) We compute numerical solution of differential equation (6) for $\alpha = 1$ and $\gamma = 1$ using finite difference method (46.1)–(46.2) for uniform mesh and compare our results with the quintic B-spline collocation method discussed by Mittal and Arora [20] and the lattice Boltzmann method proposed by Lai and Ma [17]. The exact solution of (6) for the above parameters is

$$u(x,t) = b + \frac{15}{19}\sqrt{\frac{11}{19}}(-9\tanh(K(x - bt - x_0)) + 11\tanh^3(K(x - bt - x_0))).$$

For numerical computation, we choose the same theoretical parameters as in [17, 20]: $b = 5$, $K = \frac{1}{2}\sqrt{\frac{11}{19}}$, $x_0 = -12$ and the solution domain is taken as $[-30, 30]$ with

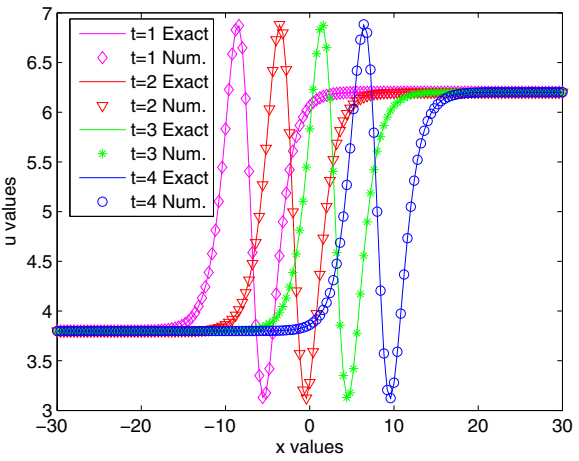

Fig. 6 Example 4: Comparison between numerical and exact solution at different times

Table 6 Comparison of global relative error in u for Example 5 with change in number of partitions at different times

t	$N+1=200$		$N+1=300$		$N+1=400$	
	$O(k^2+h^4)$-method (46.1)–(46.2)	Method discussed in [20]	$O(k^2+h^4)$-method (45.1)–(45.2)	Method discussed in [20]	$O(k^2+h^4)$-method (45.1)–(45.2)	Method discussed in [20]
1	3.3445(−05)	2.1335(−04)	2.4382(−05)	1.2335(−04)	2.2991(−05)	6.6956(−05)
2	5.8065(−05)	3.0874(−04)	4.4914(−05)	1.6780(−04)	4.2944(−05)	9.6417(−05)
3	7.9875(−05)	3.9500(−04)	6.4010(−05)	2.0791(−04)	6.1833(−05)	1.0947(−04)
4	9.7756(−05)	4.8479(−04)	8.1239(−05)	2.5018(−04)	7.9068(−05)	1.2600(−04)

number of partitions as 150 and $k = 0.01$. To test the accuracy of the method, we have computed the global relative error defined using the formula

$$\text{GRE} = \frac{\sum_{l=1}^{N} |u(x_l, t) - u^*(x_l, t)|}{\sum_{l=1}^{N} |u^*(x_l, t)|}.$$

The global relative errors for the solution of KS equation are listed in Table 5 at different times $t = 1, 2, 3$, and 4. We show the two-dimensional visual comparison of exact and numerical solution at different times in Fig. 6. In Table 6, the global relative error is compared for different number of partitions for various time intervals with those of [20] to present the effect of change in the number of mesh points.

Example 6 (*Kuramoto-Sivashinsky equation with* $\alpha = -1$ *and* $\gamma = 1$) The exact solution of the KS equation (6) with $\alpha = -1$ and $\gamma = 1$ is given by

$$u(x,t) = b + \frac{15}{19\sqrt{19}}(-3\tanh(K(x - bt - x_0)) + \tanh^3(K(x - bt - x_0))).$$

For numerical computation, we choose the same physical constants as in [17, 20]: $b = 5$, $K = \frac{1}{2\sqrt{19}}$, $x_0 = -25$ and the solution domain is taken as $[-50, 50]$ with

Table 7 Comparison of global relative error in u for the KS equation (6), Example 6 with $\alpha = -1$ and $\gamma = 1$ at different times

t	$O(k^2+h^4)$-method (46.1)–(46.2)	Method discussed in [20]	Method discussed in [17]
6	8.9929(−08)	6.5093(−06)	7.8808(−06)
8	2.3011(−07)	7.1315(−06)	9.5324(−06)
10	3.3576(−07)	7.3103(−06)	1.0891(−05)
12	5.2537(−07)	8.7766(−06)	1.1793(−05)

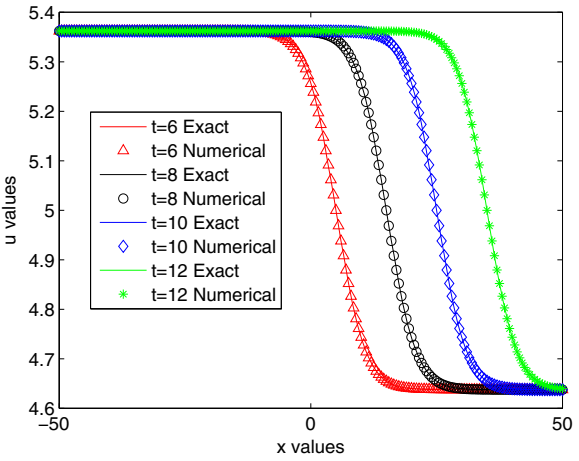

Fig. 7 Example 5: Comparison between numerical and exact solution at different times

number of partitions as 200 and $k = 0.01$. In Table 7, we present a comparison of the global relative error found by method (46.1)–(46.2) with the B-spline collocation method of [20] and the lattice Boltzmann method of [17]. The two-dimensional graph of numerical solution vs. exact solution is plotted in Fig. 7 for $-50 < x < 50$.

Example 7 (*Generalized Kuramoto-Sivashinsky equation*) Equation (5) is also known as KdV-Burgers-Kuramoto equation. For $\beta = 0$, (5) is the KS equation. We compute numerical solution of differential equation (5) for $\alpha = 1, \beta = 4$ and $\gamma = 1$ using finite difference method (46.1)–(46.2) for uniform mesh and compare our results with the lattice Boltzmann method discussed in [17]. The exact solution of (5) for the above parameters is

$$u(x,t) = b + 9 - 15(\tanh(K(x - bt - x_0)) + \tanh^2(K(x - bt - x_0)) - \tanh^3(K(x - bt - x_0))).$$

For numerical computation, we choose the same theoretical parameters as in [17]: $b = 6$, $K = \frac{1}{2}$ and $x_0 = -10$ and the solution domain is taken as $[-30, 30]$ with $h = 0.1$, $k = 0.0001$. To test the accuracy, the global relative error is compared in

Table 8 Comparison of global relative error in u for the GKS equation (5), Example 7 with $\alpha = 1$, $\beta = 4$ and $\gamma = 1$ at different times

t	$O(k^2 + h^4)$-method (46.1)–(46.2)	Method discussed in [17]
1	8.4059(−05)	2.5945(−02)
2	2.7154(−04)	2.7959(−02)
3	5.3351(−04)	2.6701(−02)
4	8.5210(−04)	3.5172(−02)

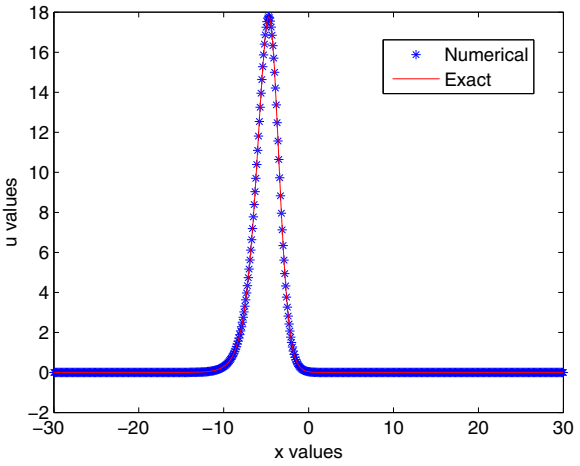

Fig. 8 Example 6: Comparison between numerical and exact solution at $t = 1$

Table 8 at time $t = 1, 2, 3$, and 4. In Fig. 8, two-dimensional comparison of exact and numerical solution is presented at $t = 1$.

Example 8 (*Extended Fisher-Kolmogorov equation*)

$$\frac{\partial u}{\partial t} + \gamma \frac{\partial^4 u}{\partial x^4} - \frac{\partial^2 u}{\partial x^2} + f(u) = \phi(x,t), \quad 0 < x < 1, \quad t > 0, \tag{65}$$

where $f(u) = u^3 - u$ (see Khiari and Omrani [14]). Here

$$\phi(x,t) = \left(16\gamma\pi^4 + 4\pi^2 + e^{-2t}\sin^2(2\pi x) - 2\right)e^{-t}\sin(2\pi x).$$

The exact solution of the above problem for $\gamma = 0.1$ is $u(x,t) = e^{-t}\sin(2\pi x)$. The numerical solution of differential equation (64) is computed using finite difference method (46.1)–(46.2) for uniform spatial mesh with number of partitions 8, 16, 32,

Table 9 The root mean square error, the maximum absolute error and the order of convergence of method (46.1)–(46.2) for Example 8 at $t = 1$ and 2 for a fixed $\lambda = (k/h^2) = 1.6$ (uniform mesh)

	$t = 1$				$t = 2$			
h	RMSE	Order	MAE	Order	RMSE	Order	MAE	Order
1/8	7.9824(−04)	–	1.0560(−03)	–	2.9407(−04)	–	3.8902(−04)	
1/16	4.7263(−05)	4.0780	6.4717(−05)	4.0283	1.7412(−05)	4.0780	2.3842(−05)	4.0283
1/32	2.8921(−06)	4.0305	4.0259(−06)	4.0068	1.0655(−06)	4.0305	1.4832(−06)	4.0067
1/64	1.7924(−07)	4.0122	2.5184(−07)	3.9987	6.5990(−08)	4.0131	9.2806(−08)	3.9984

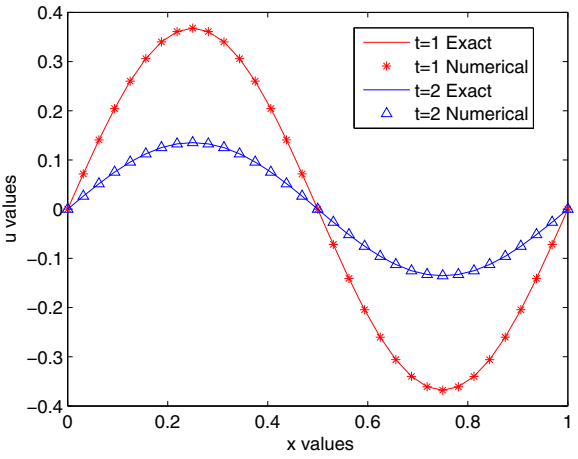

Fig. 9 Example 7: Comparison between numerical and exact solution at $t = 1$ and $t = 2$

and 64 at time $t = 1$ and 2. The maximum absolute error and the root mean square error defined using the formula

$$\text{RMSE} = \Big[\frac{1}{N}\sum_{l=1}^{N}(u(x_l,t) - u^*(x_l,t))^2\Big]^{1/2},$$

are computed. For each spatial mesh length h, the corresponding time step size is chosen as $k \propto h^2$. With this choice of time step size, the theoretical order of convergence becomes $O(h^4)$, i.e., the method is fourth-order accurate in space, which is verified using the formula $(\log(e_{h_1}) - \log(e_{h_2}))/(\log(h_1) - \log(h_2))$, where e_{h_1} and e_{h_2} are errors corresponding to two uniform mesh lengths h_1 and h_2, respectively. The root mean square error, the maximum absolute error and the order of convergence are tabulated in Table 9. Figure 9 shows the two-dimensional visual comparison of the exact and numerical solutions at $t = 1$ and 2.

The above examples have been taken to demonstrate the effect and utility of the proposed methods. These numerical experiments show that the obtained results are not only quite satisfactory with respect to the exact solutions but are also much more accurate than the solutions described in the available literature. We have solved Examples 1, 2, and 4 with variable mesh methods of $O(k^2+kh_l+h_l^3)$ and $O(k^2+h_l^2)$ with $N + 1 = 8,\ 16$, and 32 and the maximum absolute errors are reported for each case in Tables 1, 2, and 4, respectively. It is observed from these tables that the error decreases as the number of subintervals $N + 1$ increases.

6 Final discussion

In this paper, we have developed two new implicit variable mesh difference schemes for the solution of 1D unsteady quasi-linear biharmonic problem of second kind

based on Numerov type discretization using coupled approach. The proposed difference methods use only three spatial grid points x_l, $x_{l\pm1}$ of a single computational cell and no fictitious points for incorporating the boundary conditions are required. The methods are shown to be stable for all values of the mesh ratio parameter $\lambda = k/h^2$ for uniform mesh. We present stable difference schemes for a class of one space unsteady linear singular biharmonic problem by modifying the proposed schemes in such a way that the solution retains its order and accuracy everywhere including the region in the vicinity of the singularity without using any fictitious points outside the solution region to handle the numerical scheme near the boundary. The numerical solution of u_{xx} is determined as a by-product of the methods, which is quite often of interest in various applied mathematics problems. The results of a number of numerical experiments on problems of physical importance are presented to illustrate the effectiveness and efficiency of the proposed methods. The numerical results clearly indicate that the methods produce better results in comparison with the existing methods of Mittal and Arora [20] and Lai and Ma [17] for the classical nonlinear Kuramoto-Sivashinsky equation. It is noted from Tables 5, 6, 7, and 8 that the accuracy of the solution for the KS equation decreases with time due to the time truncation errors of the time derivative term. We observe from Table 9 that the uniform mesh discretization produces fourth-order accurate results for a fixed mesh ratio parameter λ for the extended Fisher-Kolmogorov equation. The graphical representation of numerical solution at various time intervals exhibits the same characteristics as existing in the literature. The proposed methods are easily implemented, concise, and approximate the exact solution very well for a large class of nonlinear PDEs. It is hopeful that the presented methods will help in solving other nonlinear unsteady biharmonic problems in applied sciences and engineering. Further research will be directed to extend the proposed methods to solve 2D unsteady biharmonic problems.

Acknowledgments The authors thank the reviewers for their valuable suggestions, which substantially improved the standard of the paper.

References

1. Aronson, D.G., Weinberger, H.F.: Multidimensional nonlinear diffusion arising in population genetics. Adv. in Math **30**, 33–67 (1978)
2. Conte, R.: Exact Solutions of Nonlinear Partial Differential Equations by Singularity Analysis, Lecture Notes in Physics, pp. 1–83. Springer, Berlin (2003)
3. Danumjaya, P., Pani, A.K.: Orthogonal cubic spline collocation method for the extended Fisher-Kolmogorov equation. J. Comput. Appl. Math **174**, 101–117 (2005)
4. Dee, G.T., Van Saarloos, W.: Bistable systems with propagating fronts leading to pattern formation. Phys. Rev. Lett. **60**, 2641–2644 (1988)
5. Doss, L.J.T., Nandini, A.P.: An H^1-Galerkin mixed finite element method for the extended Fisher-Kolmogorov equation. Int. J. Numer. Anal. Model. Ser. B **3**, 460–485 (2012)
6. Fan, E.: Extended tanh-function method and its applications to nonlinear equations. Phys. Lett. A **277**, 212–218 (2000)
7. Ganaiea, I.A., Arora, S., Kukreja, V.K.: Cubic Hermite collocation solution of Kuramoto-Sivashinsky equation. Int. J. Comput. Math **93**, 223–235 (2016)
8. Greig, I.S., Morris, J.L.: A Hopscotch method for the Kortewegde Vries equation. J. Comput. Phys. **20**, 229–236 (1976)

9. Hageman, L.A., Young, D.M.: Applied Iterative Methods. Dover Publication, New York (2004)
10. Hooper, A.P., Grimshaw, R.: Nonlinear instability at the interface between two viscous fluids. Phys. Fluids **28**, 37–45 (1985)
11. Kaya, D.: An application for the higher order modified KdV equation by decomposition method. Commun. Nonlinear Sci. Numer. Simul. **10**, 693–702 (2005)
12. Kelly, C.T.: Iterative Methods for Linear and Non-linear Equations. SIAM Publications, Philadelphia (1995)
13. Khater, A.H., Temsah, R.S.: Numerical solutions of the generalized Kuramoto-Sivashinsky equation by Chebyshev spectral collocation methods. Comput. Math. Appl. **56**, 1465–1472 (2008)
14. Khiari, N., Omrani, K.: Finite difference discretization of the extended Fisher-Kolmogorov equation in two dimension. Comput. Math. Appl. **62**, 4151–4160 (2011)
15. Korteweg, D.J., de Vries, G.: On the change of form of long waves advancing in a rectangular canal, and on a new type of long stationary waves. Philos. Mag. **39**, 422–443 (1895)
16. Kuramoto, Y., Tsuzuki, T.: Persistent propagation of concentration waves in dissipative media far from thermal equilibrium. Prog. Theor. Phys. **55**, 356–369 (1976)
17. Lai, H., Ma, C.: Lattice Boltzmann method for the generalized Kuramoto-Sivashinskyequation. Phys. A **388**, 1405–1412 (2009)
18. Lakestani, M., Dehghan, M.: Numerical solutions of the generalized Kuramoto-Sivashinsky equation using B-spline functions. Appl. Math. Model **36**, 605–617 (2012)
19. Mitchell, A.R.: Computational Methods in Partial Differential Equations. Wiley, New York (1969)
20. Mittal, R.C., Arora, G.: Quintic B-spline collocation method for numerical solution of the Kuramoto-Sivashinsky equation. Commun. Nonlinear Sci. Numer. Simul. **15**, 2798–2808 (2010)
21. Mohanty, R.K.: An accurate three spatial grid-point discretization of $O(k^2 + h^4)$ for the numerical solution of one-space dimensional unsteady quasi-linear biharmonic problem of second kind. Appl. Math. Comput. **140**, 1–14 (2003)
22. Mohanty, R.K., Kaur, D.: High accuracy implicit variable mesh methods for numerical study of special types of fourth order non-linear parabolic equations. Appl. Math. Comput. **273**, 678–696 (2016)
23. Saad, Y.: Iterative Methods for Sparse Linear Systems. SIAM Publisher (2003)
24. Saprykin, S., Demekhin, E.A., Kalliadasis, S.: Two-dimensional wave dynamics in thin films. I. Stationary solitary pulses. Phys. Fluids **17**, 117105 (2005)
25. Sivashinsky, G.I.: Instabilities, pattern-formation, and turbulence in flames. Annu. Rev. Fluid Mech. **15**, 179–199 (1983)
26. Taha, T.R., Ablowitz, M.J.: Analytical and numerical aspects of certain nonlinear evolution equations. III. Numerical, Kortewegde Vries equations. J. Comput. Phys. **55**, 231–253 (1984)
27. Tatsumi, T.: Irregularity, regularity and singularity of turbulence. Turbulence and chaotic phenomena in fluids. Iutam, 1–10 (1984)
28. Uddin, M., Haq, S., Siraj-ul-Islam.: A mesh-free numerical method for solution of the family of Kuramoto-Sivashinsky equations. Appl. Math. Comput. **212**, 458–469 (2009)
29. Vliegenthart, A.C.: On finite difference methods for the Korteweg-de Vries equation. J. Eng. Math **5**, 137–155 (1971)
30. Xu, Y., Shu, C.W.: Local discontinuous Galerkin methods for the Kuramoto-Sivashinsky equations and the Ito-type coupled KdV equations. Comput. Methods Appl. Mech. Engrg. **195**, 3430–3447 (2006)
31. Zhu, G.: Experiments on director waves in nematic liquid crystals. Phys. Rev. Lett. **49**, 1332–1335 (1982)